FINAL REPORT

Refinement and Validation of Empirical Techniques for the Determination of Absorption Coefficients for Marine Particulates

B. Greg Mitchell, Principal Investigator
Assistant Research Biologist
Marine Research Division, 0218
Scripps Institution of Oceanography
University of California, San Diego
La Jolla, California 92093-0218

ONR Grant N00014-89-J-1071

Overview of ONR sponsored research to Dr. B. Greg Mitchell, and long-range goals

A thorough understanding of marine optics is a mission of significant Naval relevance. The ability to use optical measurements (in situ and remote) to estimate light propagation and phytoplankton growth rates is a significant objective. This objective requires a detailed understanding of the nature and variability of source and loss terms, and an ability to model the relevant rates. Figure 1 summarizes dominant state variables and transformations occurring in marine optics, and the contributions by the principal investigator in understanding these processes. Several significant problems previously have not been resolved with respect to measuring or modeling the processes in Figure 1. The long-range objectives of the principal investigator is to continue studies of the various components and rate processes shown in Figure 1 in an effort to improve our understanding of marine optical properties and photo-physiology and ecology of phytoplankton.

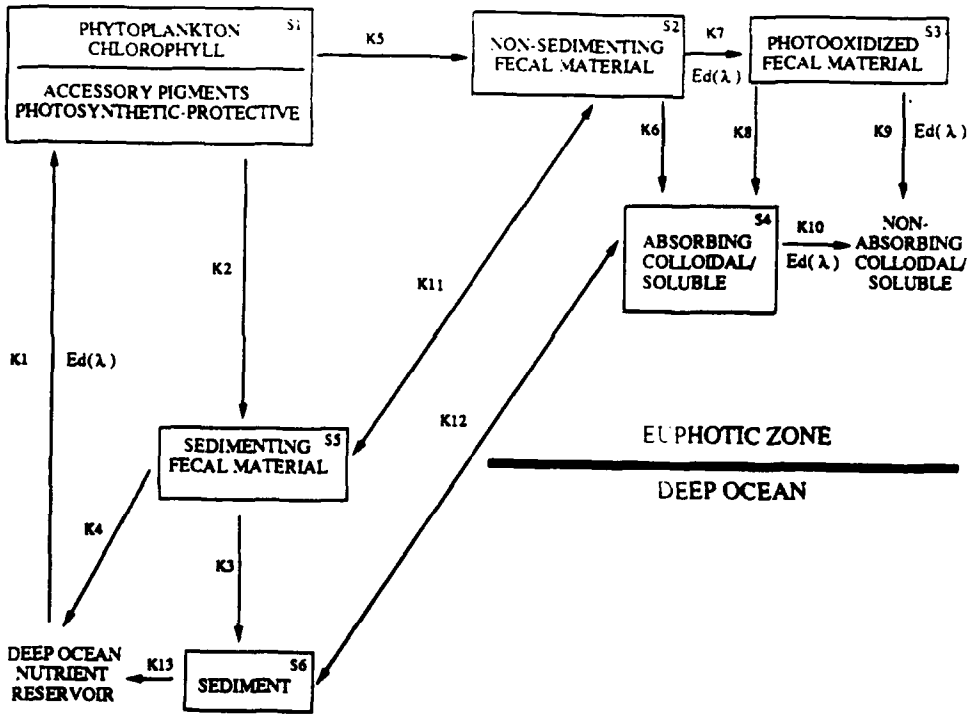

Figure 1. A conceptual model of optically important processes in the ocean. The long-range objectives of our research include a detailed understanding of the processes and state variables specified in this figure. The state variables in the boxes (S1-S6) correspond to dominant sources of optical variability in the oceans. The principal investigator has dedicated his research effort to understanding the diverse aspects of this system. Methods for estimating the magnitude and characteristics of S1, S2 and S3 have included analysis of particle absorption using microphotometry (Iturriaga et al., 1988); macrophotometry (Mitchell and Kiefer, 1984; Mitchell et al. 1984; Mitchell and Kiefer, 1988a; 1988b; Mitchell, 1990); in situ optical profiling resulting in discovery of regional bio-optical relationships (Mitchell and Holm-Hansen, 1991a; Mitchell, 1992); a novel method to estimate S1 from moored radiometers (Stramski et al. 1992); and aircraft (Tanis et al., 1990) or satellite observations of biomass (Mitchell et al., 1991). Optical based models of phytoplankton photosynthesis for laboratory cultures (Kiefer and Mitchell, 1983; Sosik and Mitchell, 1991) for Antarctic phytoplankton (Mitchell and Holm-Hansen, 1991b) and for Arctic phytoplankton (Cota et al., 1992) have been developed to model process K1. Siegel et al. (1989) used an *in situ* optical approach to estimate K1 and K2+K5 for populations in the North Pacific Gyre. Carder et al. (1991) have used optical methods to partition S1 from S2 and S3 for remote sensing. Sedimentation rates of Antarctic and Arctic phytoplankton (K2) have been studied by Mitchell and Holm-Hansen (1991b) and Wassman et al., (1990).

Publications by the PI contributing to understanding ocean optics as described in Figure 1. Citations with a double asterisk (**) were sponsored by grant N00014-89-J-1071; those with a single asterisk (*) were sponsored by ONR support since 1982.

* Carder, K. L., S. K. Hawes, K. A. Baker, R. C. Smith, R. G. Steward, B. G. Mitchell (1991) Reflectance model for quantifying chlorophyll a in the presence of productivity degradation products. Journal of Geophysical Research, 96(C11):20,599-20611.

* Cota, G. F, G. G. Mitchell, W. O. Smith, Jr. (1992) Photophysiology of *Phaeocystis pouchetti* in the Greenland Sea. In preparation.

* Iturriaga, R., B. G. Mitchell, D. A. Kiefer. 1988. Microphotometric analysis of individual particle absorption spectra. Limnology and Oceanography, 33(1):128-135.

Kiefer D. A. and B. G. Mitchell (1983) A simple, steady state description of phytoplankton growth based on absorption cross section and quantum efficiency. Limnology and Oceanography, 28, 770-776.

* Mitchell, B. G. and D. A. Kiefer (1984) Determination of absorption and fluorescence excitation spectra for phytoplankton. In Marine Phytoplankton and Productivity, O. Holm-Hansen, L. Bolis, and R. Gilles, Eds. Springer-Verlag, Berlin.

* Mitchell, B.G., R. Iturriaga, and D.A. Kiefer, 1984, Variability of spectral absorption coefficients in the Eastern Pacific Ocean. In Ocean Optics VII, Marvin Blizard, ed. Proc. Soc. Photo-Optical Instrumentation Engineers. 489: 113-118.

* Mitchell B. G. and D. A. Kiefer (1988a) Chlorophyll a specific absorption and fluorescence excitation spectra for light-limited phytoplankton. Deep-Sea Research, 35, 639-663.

* Mitchell B. G. and D. A. Kiefer (1988b) Variability in pigment specific particulate fluorescence and absorption spectra in the North Eastern Pacific Ocean. Deep-Sea Research, 35, 665-689.

** Mitchell B. G. (1990) Algorithms for determining the absorption coefficient of aquatic particulates using the Quantitative Filter Technique (QFT). Ocean Optics X. SPIE 1302: 137-148.

* Mitchell, B. G. (1992) Predictive bio-optical relationships for polar oceans and marginal ice zones. Journal of Marine Systems. In press.

Mitchell, B. G. and O. Holm-Hansen (1991a) Bio-optical properties of Antarctic waters: Differentiation from temperate ocean models. Deep Sea Research, 38(8/9): 1009-1028.

Mitchell, B. G. and O. Holm-Hansen (1991b) Observations and modeling of the Antarctic phytoplankton crop in relation to mixing depth. Deep-Sea Research, 38(8/9): 981-1007.

* Mitchell, B. G., E. B. Brody, E-N. Yeh, C. McClain, J. Comiso and N. G. Maynard (1991) Meridional zonation of the Barents Sea ecosystem inferred from satellite remote sensing and in situ bio-optical observations. Polar Research. In press.

* Siegel, D. A., T. D. Dickey, L. Washburn, M. K. Hamilton and B. G. Mitchell (1989) Optical determination of particulate abundance and production variations in the oligotrophic ocean. Deep-Sea Research, 36:211-222.

** Sosik, H. M. and B. G. Mitchell (1991) Absorption, fluorescence, and quantum yield for growth in nitrogen-limited Dunaliella tertiolecta. Limnology and Oceanography, 326(5):910-922.

* Stramski, D. C., R. Booth and B. G. Mitchell (1992) Estimation of downward irradiance attenuation from a single moored instrument. Deep-Sea Research. In press.

* Tanis, F., T. O. Manley and B. G. Mitchell (1990) Helicopter and ship-based measurements of mesoscale ocean color and thermal features in the marginal ice zone. Ocean Optics X. R. Spinrad, Ed. SPIE 1302:225-237.

Wassmann, P., M. Vernet, B. G. Mitchell and F. Rey (1990) Mass sedimentation of Phaeocystis pouchetti in the Barents Sea. Marine Ecology Progress Series, 63:183-195.

OBJECTIVES FOR GRANT N00014-J-1071

The work completed with support of N000-14-J-1071 was carried out to improve our ability to measure the light absorption by the particles contained in the boxes labeled S1, S2 and S3 in Figure 1. The principal goal of the work in FY89 was to develop and validate a simple, practical and accurate procedure for determination of particulate absorption coefficients (a_p) for samples concentrated onto glass fiber filters (Quantitative Filter Technique, QFT). Included in this effort was an analysis of the reproducibility, limitations and statistical precision of the methods and a theoretical treatment of empirical results.

TASKS COMPLETED

During FY89 a detailed study was initiated to evaluate the ability to determine a_p for dilute suspensions of pigmented particles (e.g. sea water) using the QFT. A Perkin-Elmer Lambda 6 High Performance spectrophotometer with a dual grating monochromator and an integrating sphere attachment was purchased to conduct the work. The QFT, integrating sphere and opal glass procedures were compared for various species of phytoplankton in culture. The integrating sphere attachment allows direct determination of a_p for suspensions. Different glass fiber filter types and particle types were analyzed and empirical algorithms were determined for correction of the path length aplification factor (Beta) which is caused by light scattering in the glass fiber medium.

Experiments to determine the pathlength amplification factor for various filter types was completed. Empirical algorithms were determined and optimized. The absolute transmittance, reflectance and absorbtance for different samples and densities was measured for comparison with theoretical models of absorption by turbid samples.

The dependence of Beta on sample density was confirmed; the source of significant variance in Beta is under review. A previous optimized algorithm for GF/F filters (Mitchell and Kiefer, 1988) yields a_p which are reproducible within 15% and which agree with the integrating sphere results within 15%. New algorithms for several different types of filters have been developed and have been published (Mitchell, 1990).

We have carried out a detailed evaluation of the generality, precision and accuracy of the Quantitative Filter Technique (QFT) for determination of absorption coefficients of aquatic particulates (Mitchell, 1990). The theoretically predicted (Mitchell and Kiefer, 1988a) non-linear nature of absorption pathlength amplification for particles retained on intensely scattering filters was confirmed and a new, more direct algorithm for correction was developed. Briefly, the method was shown to have (i) general utility such that raw absorbance determined on different spectrophotometers is comparable; (ii) a precision of better than $\pm$ 10% for determinations on replicates; and (iii) an accuracy of better than $\pm$ 15% for algorithms determined for a specified lot of filters. However, variability in different filter lots of the same filter type can cause an additional error of $\pm$ 10-15% if correction algorithms are not determined for the lot of filters used.

PUBLICATIONS ACKNOWLEDGING N00014-89-J-1071. Copies included with report.

Mitchell, B. G. 1990: Algorithms for quantitative determination of absorption coefficients for aquatic particulates concentrated on filters. Ocean Optic X. SPIE 1302:137-148.

Sosik, H. M. and B. G. Mitchell. 1991 Absorption, fluorescence, and quantum yield for growth in nitrogen-limited Dunaliella tertiolecta. Limnology and Oceanogrphy. 36(5): 910-921.

Limnol. Oceanogr., 36(5), 1991, 910–921

Absorption, fluorescence, and quantum yield for growth in nitrogen-limited *Dunaliella tertiolecta*

Heidi M. Sosik and B. Greg Mitchell
Marine Research Division, 0218, Scripps Institution of Oceanography, UCSD, La Jolla, California 92093

Abstract

The effects of steady state nitrogen limitation on the optical properties of *Dunaliella tertiolecta* were investigated. Growth rate was varied in a continuous culture under constant irradiance and temperature with absorption, fluorescence, and cellular characteristics including pigment contents determined at each steady state. The cellular concentration of Chl *a* increased with growth rate while Chl-*a*-specific absorption and fluorescence both decreased. In addition, the quantum yield for growth varied by more than a factor of 3.5 over the growth conditions examined, with the highest yield in the most rapidly growing cells. The decrease in magnitude of Chl-*a*-specific optical properties is caused by pigment package effects and changes in the abundance of accessory pigments relative to Chl *a*. Changes in absorption and fluorescence properties are consistent with theoretical predictions for discrete packages. In addition, pigment-based reconstruction techniques overestimate the magnitude of both in vivo and unpackaged absorption by *D. tertiolecta* under these growth conditions. The observed variability in Chl-*a*-specific absorption and quantum yield is a fundamental aspect of phytoplankton physiology that should be incorporated into models of oceanic primary production.

Optical measurements from in situ profiling instruments, moorings, aircraft, and satellites provide information at temporal and spatial scales not possible with traditional biological oceanographic techniques. The potential for this information to enhance understanding of primary productivity in the ocean depends on models that relate optical properties to photosynthesis. Although bio-optical models for primary production and phytoplankton growth have been developed and are being evaluated (Bannister 1979; Kiefer and Mitchell 1983; Smith et al. 1989), an increased knowledge of the sources and magnitude of variability in the parameters of these models is critical for accurate assessment of modeling capabilities.

An important component of these models involves prediction of photosynthetic production or growth from light and chlorophyll data. Variability in this relationship may be caused by changes in Chl *a*-specific absorption or changes in the quantum yield of photosynthesis. The spectral Chl-specific absorption coefficient, $a_{ph}^*(\lambda)$ (units given in list of notation), is an important parameter of the models; it provides an estimate of the amount of light absorbed by phytoplankton cells from knowledge of ambient irradiance and Chl *a* concentration. The photosynthetic quantum yield, ϕ_{ph}, is the efficiency with which the absorbed light is used for C fixation. Knowledge of the variability in these physiological parameters with growth conditions is important in accurately applying bio-optical models to diverse oceanographic regions and conditions.

Modeling primary production over large scales also relies on estimates of pigment data from remote sensing. The accuracy of current algorithms for retrieving phytoplankton pigment concentrations from optical data is limited by lack of knowledge concerning the variability in pigment-specific light absorption. This variability includes both changes in $a_{ph}^*(\lambda)$ and changes in the relative importance of phytoplankton, detritus, and dissolved material as absorbers in the water column (e.g. Morel 1988; Mitchell and Holm-Hansen 1991). Thus physiological variability in pigment-specific absorption can potentially be important in estimating the biomass of primary produc-

Acknowledgments

This work was supported in part by ONR contract N00014-89-J-1071 to B.G.M. and an NSF graduate fellowship to H.M.S.

We thank R. R. Bidigare for the HPLC analysis of pigments and J. Kitchen for providing technical specifications on the spectral characteristics of the Sea Tech fluorometer.

Notation

$a_{ph}(\lambda)$, $a_{Tr}(\lambda)$, $a_{sol}(\lambda)$	Absorption coefficient for phytoplankton in vivo, after solubilization in 0.5% Triton X-100, and for intracellular material, m^{-1}
$a_{ph}^*(\lambda)$, $a_{Tr}^*(\lambda)$, $a_{sol}^*(\lambda)$, $a_{int}^*(\lambda)$	Chl *a*-specific absorption coefficient for phytoplankton in vivo, after solubilization in 0.5% Triton X-100, for a solution of cell material, and for intracellular material, m^2 (mg Chl *a*)$^{-1}$
$a_i^*(\lambda)$	Specific absorption coefficient for pigment *i*, m^2 (mg pigment *i*)$^{-1}$
$b_b(\lambda)$	Backscatter coefficient, m^{-1}
c	Intracellular concentration of Chl *a*, mg m^{-3}
C_i	Concentration of pigment *i* in a cell suspension, mg m^{-3}
d	Cell diameter, μm
$D(\lambda)$, G	Detection or geometric constant, dimensionless
$E_0(\lambda)$	Growth irradiance, mol quanta m^{-2} d^{-1} nm^{-1}
$E(\lambda)$	Fluorescence excitation irradiance, mol quanta m^{-2} s^{-1} nm^{-1}
F	Fluorescence from a single cell, quanta s^{-1}
$\bar{F}$	Broadband fluorescence per cell, relative quanta s^{-1} $cell^{-1}$
$\bar{F}^*$	Broadband fluorescence per Chl *a*, relative quanta s^{-1} (mg Chl *a*)$^{-1}$
$Q_a(\lambda)$	Absorption efficiency, dimensionless
$Q_a^*(\lambda)$	Packaging parameter, dimensionless
λ_e, λ_f	Wavelength of excitation light and fluoresced light, nm
μ	Specific growth rate (base *e*), d^{-1}
ϕ_{ph}, $\phi\mu$	Quantum yield for photosynthesis and growth, mol C (mol quanta)$^{-1}$
ϕ_f	Quantum yield for fluorescence, mol quanta fluoresced (mol quanta absorbed)$^{-1}$
ρ'	Optical thickness along the particle diameter, dimensionless

ers as well as the production realized by that biomass.

Chl *a*-specific absorption at the blue peak and ϕ_{ph} have been shown to vary in laboratory cultures by at least fourfold and tenfold, respectively. Differences in $a_{ph}^*(\lambda)$ among species have been observed, and variability within species caused by changes in growth irradiance has been well documented. This variability in $a_{ph}^*(\lambda)$ is attributed in part to pigment packaging effects that vary with cell size and pigment content per cell (Morel and Bricaud 1981; Mitchell and Kiefer 1988) as well as changes in the abundance of accessory pigments relative to Chl *a* (Bricaud et al. 1983; Sathyendranath et al. 1987; Berner et al. 1989). In addition to variability in $a_{ph}^*(\lambda)$, there are differences in ϕ_{ph} among species and as a function of growth irradiance for a single species (Kiefer and Mitchell 1983; Falkowski et al. 1985; Sakshaug et al. 1989).

Other factors besides light can lead to physiological adaptations that result in variability in the optical properties of phytoplankton cells. Chl *a*-specific absorption and quantum yield have been shown to be affected by N depletion in batch cultures (Welschmeyer and Lorenzen 1981; Cleveland and Perry 1987). The physiological effects of starvation may be quite different, however, from those observed under steady state nutrient limitation in continuous culture. Although $a_{ph}^*(\lambda)$ can vary under steady state N-limited growth, Kiefer and Mitchell (1983) hypothesized that there should be no effect on ϕ_{ph}. Recent studies of phytoplankton in N-limited continuous culture have shown significant variability in both $a_{ph}^*(\lambda)$ and ϕ_{ph} (Chalup and Laws 1990; Herzig and Falkowski 1989). Before the effects of physiological variability on bio-optical modeling of primary production can be evaluated, a more complete characterization of this variability and its sources is necessary.

In vivo fluorescence is another optical property widely used to characterize primary producers in the ocean. Measurements can be made rapidly over a range of scales. Accurate assessment of phytoplankton biomass is limited, however, by variability in the relationship between in vivo fluorescence and other variables like Chl *a* concentration. Previous studies of laboratory cultures have documented that for a single species fluorescence per Chl *a* varies with growth conditions such as light and nutrient availability (e.g. Kiefer 1973; Mitchell and Kiefer 1988; Sosik et al. 1989), but further investigations into the sources of this variability are necessary to reliably interpret fluorescence signals from natural samples.

In this work, we have examined the effects of steady state NO_3^--limited growth on pigmentation, absorption, and fluorescence in the marine chlorophyte *Dunaliella terti-*

olecta. The roles of pigment packaging and pigment composition in determining light utilization efficiency have been considered and the results placed in the context of theoretical work on absorption and fluorescence by single cells.

Materials and methods

Dunaliella tertiolecta Butcher (FCRG culture collection) was maintained in NO_3^--limited continuous culture at four dilution rates. The vessel was kept at 22°C; sterile GPM media (Loeblich 1975) at full strength except with 40 μM NO_3^- was used for dilution, and the cultures were stirred continuously and bubbled with sterile, water-saturated air. Constant light was provided with "cool-white" fluorescent lamps at an irradiance of 165 μmol quanta m^{-2} s^{-1} for all dilution rates. Light intensity was measured with a Biospherical Instruments QSL-100 quantum scalar irradiance meter. Absolute spectral irradiance was determined from these measurements and the relative spectrum for "cool-white" lamps provided by General Electric. In each case, analysis was conducted when fluorescence of the cell suspension remained constant for at least 2 d and always after at least 10 d at a constant dilution rate. Specific growth rate μ (base e) was determined as the dilution rate of the culture (flow rate divided by the culture volume).

Subsamples of the cell suspensions were filtered onto Whatman GF/C glass-fiber filters and stored immediately at −70°C in cryotubes flushed with N_2 gas. These samples were later analyzed for pigments by reverse-phase, high-performance liquid chromatography (HPLC) following the methods described by Bidigare (1989). Additional samples were filtered onto previously combusted GF/C filters and frozen in combusted Pyrex test tubes. After desiccation of these samples, carbon and nitrogen contents were measured with a Perkin Elmer P-E 2400 CHN elemental analyzer. Cell density and equivalent spherical cell volume were determined on a Coulter Electronics 64-channel, model ZH electronic particle counter. After 15 min of dark incubation, fluorescence of the cell suspension was measured on a Turner Designs model 10 fluorometer. Bulk fluorescence was also measured with a Sea Tech in situ fluorometer after a dilution of ~1 : 40 with filtered seawater.

Absorption properties were determined with a dual-grating Perkin Elmer lambda 6 UV/VIS spectrophotometer equipped with an integrating sphere. Conventional spectroscopic techniques do not provide accurate measurements of absorption for particles in suspension (Shibata 1958), but the integrating sphere allows collection of light scattered by particles in the forward direction thus improving absorption estimates. Cell suspensions were concentrated about fivefold by centrifugation. In vivo spectral absorption, $a_{ph}(\lambda)$, was measured on the concentrated samples in a 1-cm cuvette. Fresh culture medium was used in the reference beam. Backscattered light is not collected by the integrating sphere, so our estimates are potentially greater than the true $a_{ph}(\lambda)$. Based on the results of Bricaud et al. (1983), however, we do not expect that the backscatter coefficient, $b_b(\lambda)$, was ever >1% of $a_{ph}(\lambda)$. Absorption was also measured on unconcentrated cell suspensions, but spectra were found to be noisy for optical densities <0.02. Comparison of the magnitude of peak absorption before and after concentration showed a linear increase with concentration factor, which was calculated from cell densities determined with the Coulter counter.

In addition to determining in vivo absorption, we treated a subsample of the concentrated suspension with the detergent Triton X-100 at a final concentration of 0.5%, with subsequent sonication. This treatment disrupts the cells and thylakoid membranes, removing pigment package effects without extraction by organic solvents (Berner et al. 1989). Spectral absorption, $a_{TX}(\lambda)$, was determined on these solubilized cells with 0.5% Triton X-100 in filtered seawater as a reference. This treatment to remove package effects should not be considered a general one as we have worked with other species and found variable success with disruption. A further limitation of the Triton X method involves spectral shifts in the wavelengths of peak absorption when compared to in vivo absorption. We have observed shifts toward shorter wavelengths of 1 nm at the

Table 1. Cellular characteristics of *Dunaliella tertiolecta* at several growth rates (base *e*) in N-limited continuous culture. Values in parentheses are 1 SD ($n = 2$ for pigments and $n = 3$ for C and N determinations). Pigments, C, and N are given in pg cell^{-1}.

	Growth rate (d^{-1})			
	0.23	0.61	1.05	2.08
Chl *a*	0.327(0.026)	0.470(0.017)	0.730(0.033)	0.763(0.025)
Chl *b*	0.095(0.010)	0.153(0.003)	0.213(0.010)	0.241(0.004)
Lutein	0.149(0.008)	0.212(0.007)	0.227(0.017)	0.281(0.006)
α-carotene	0.014(0.002)	0.013(<0.001)	0.005(0.002)	0.017(0.004)
β-carotene	0.096(0.009)	0.079(0.001)	0.075(0.018)	0.105(0.006)
Neoxanthin	0.020(0.003)	0.032(0.001)	0.042(0.003)	0.051(0.001)
Violaxanthin	0.028(0.001)	0.037(0.001)	0.057(0.004)	0.065(0.001)
Antheraxanthin	0.010(0.001)	0.010(0.001)	0.012(0.001)	0.014(0.001)
Carbon	39.68(1.41)	34.98(0.63)	26.97(0.42)	29.68(0.77)
Nitrogen	2.07(0.13)	2.33(0.09)	2.74(0.16)	2.72(0.27)
Cell diam (μm)	6.94(0.06)	6.91(n.d.)	6.45(0.15)	6.96(0.20)

blue peak and 8 nm at the red peak. To compensate for these shifts when using $a_{TX}^*(\lambda)$ in calculations or comparison with $a_{ph}^*(\lambda)$, we have shifted the spectra by 1 nm for wavelengths 350–557 nm and 8 nm for 551–750 nm. The region between 551 and 557 nm was repeated to prevent introducing a gap in the spectra; values are relatively low and uniform at these wavelengths, so this does not distort the spectra. The spectral values of $a_{TX}^*(\lambda)$, however, are presented without adjustment (*see Fig. 2B and Table 2*).

A subsample of the cell suspension was also concentrated on Whatman GF/C filters and extracted for 24 h in 90% acetone at 4°C in the dark. Spectral absorption of the extract was measured as described above except that 90% acetone was used as the reference.

Results and discussion

Cellular characteristics—As previously documented for N-limited growth of phytoplankton (e.g. Caperon and Meyer 1972; Kolber et al. 1988), we observed an increase in cellular Chl *a* as the growth rate of *D. tertiolecta* increased in the chemostat (Table 1). This more than twofold change in Chl *a* was accompanied by a corresponding increase in Chl *b* per cell (Table 1), resulting in no trend in the ratio of Chl *b* to Chl *a* (Fig. 1A). Increases were also observed in the absolute cellular concentrations of the carotenoids (Table 1). As found for Chl *b*, the amounts of the minor yellow pigments relative to Chl *a* changed very little (Fig. 1B). This constant stoichiometry is not true, however, for lutein, which decreases relative to Chl *a* at higher μ (Fig. 1A). Variability in the ratios of α- and β-carotene to Chl *a* was also observed (Fig. 1C).

The increase in Chl *a* per cell at higher dilution rate was accompanied by a parallel increase in cellular N and a decrease in cellular C (Table 1). As previously observed for this species grown under N limitation, molar C : N ratios were high and varied with growth rate (Caperon and Meyer 1972), ranging from 22 for μ of 0.23 d^{-1} to 11 at μ of 2.08 d^{-1}. In contrast to cell C, cell size did not vary systematically with μ (Table 1).

Absorption changes—Chl *a*-specific absorption in vivo, $a_{ph}^*(\lambda)$, was highest at low growth rates (Fig. 2A) that, as described above, corresponded to decreased amounts of pigment per cell. This trend also held for absorption after treatment with Triton X (Fig. 2B) and after extraction in acetone (not shown). Changes in $a_{ph}^*(\lambda)$ may be due to changes in the pigment package effect or to changes in the relative abundance of accessory pigments compared to Chl *a* (Morel and Bricaud 1981; Berner et al. 1989). Because the effect of packaging pigments in the cells and chloroplasts has been removed in the Triton X-treated samples, any changes in $a_{TX}^*(\lambda)$ should be due only to changes in the pigment composition of the cells. At the

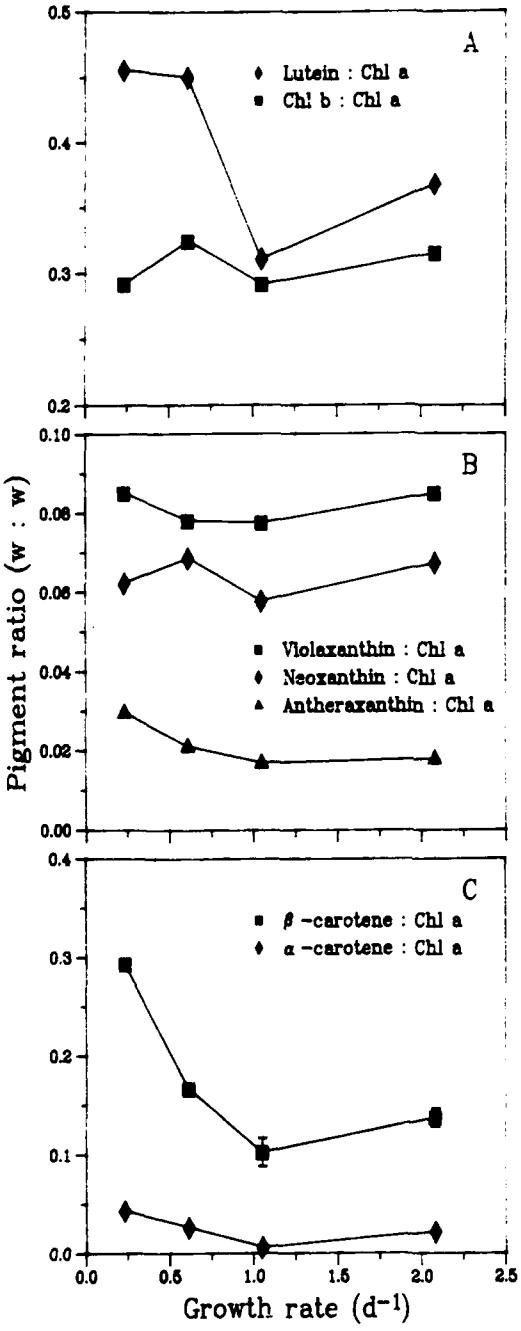

Fig. 1. Abundances of accessory pigments relative to Chl *a* as a function of growth rate in N-limited *Dunaliella tertiolecta*. Ratios for each pigment are shown with symbols identified in the panels. Standard deviations are smaller than the symbol size except where error bars are present.

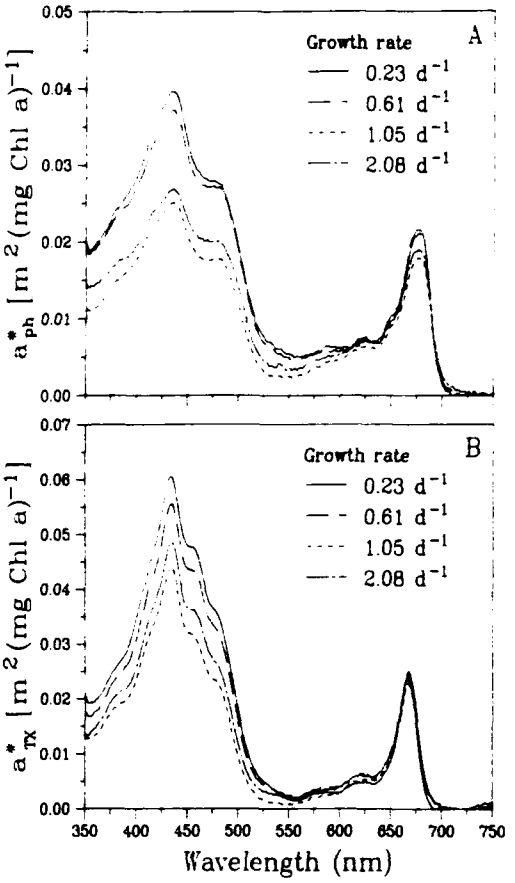

Fig. 2. Chl-*a*-specific absorption in N-limited *Dunaliella tertiolecta* at several growth rates. A. Absorption determined on whole-cell suspensions showing variability due to changes in pigmentation and pigment packaging. B. Absorption of cells disrupted by treatment with Triton X-100 so that variability is due only to changes in the abundance of accessory pigments relative to Chl *a*.

blue absorption peak, $a_{ph}^*(\lambda)$ is 48% higher at the lowest growth rate compared with the highest. In contrast, the corresponding difference for the Triton X absorption is only 24%. Because the relative variation in specific absorption without package effects is smaller than the difference in vivo, package effects and changes in pigment ratios must both contribute to variations in $a_{ph}^*(\lambda)$ with growth rate. Our results suggest that, for absorption of light at the blue peak, about half of the observed variability in $a_{ph}^*(\lambda)$ is due to package effects with the remainder caused by changes in pigment composition.

Changes in pigment composition are expected to affect specific absorption at the blue Chl *a* peak because absorption spectra for accessory pigments overlap the Chl *a* spectrum in this region. Examination of the pigment ratio data (Fig. 1) shows that response of the various accessory pigments to increased N limitation differs. It is apparent that the most important changes leading to increased $a_{TX}^*(\lambda)$ at low μ are in lutein and β-carotene relative to Chl *a*. Although the other pigments remain in fairly constant proportions to Chl *a* or are present at relatively low levels, lutein and β-carotene ratios are higher particularly at the two lowest μ. These growth rates also correspond to the highest $a_{TX}^*(\lambda)$ (Fig. 2B). In addition, at a μ of 1.05 d^{-1} the ratios are the lowest and $a_{TX}^*(\lambda)$ is also lowest.

Although changes in pigment composition play a significant role in determining in vivo absorptive properties, as the comparison of absorption for whole cells and solubilized cells indicates, the packaging of pigments into discrete particles is also important. A theoretical framework for understanding this package effect has been developed (Duysens 1956; Morel and Bricaud 1981), and its applicability for describing changes in absorption properties of light-limited algal cultures has been verified (Sathyendranath et al. 1987; Bricaud et al. 1988). Variability in $a_{ph}^*(\lambda)$ observed for nutrient-limited growth has not previously been interpreted with respect to the model of pigment packaging. In addition, an important parameter of the model, absorption by intracellular matter, $a_{cm}(\lambda)$, has remained largely uncharacterized. It is possible to estimate the magnitude and variability in $a_{cm}(\lambda)$ from Triton X absorption measurements and cellular pigment concentrations.

Theoretical work on absorption by discrete particles allows absorption efficiency as a function of wavelength, $Q_a(\lambda)$, to be predicted based on cell size and $a_{cm}(\lambda)$ (Morel and Bricaud 1981). The product of $a_{TX}^*(\lambda)$ and the intracellular concentration of Chl *a* (c) is an estimate of $a_{cm}(\lambda)$,

$$a_{cm}(\lambda) = a_{TX}^*(\lambda)\, c. \qquad (1)$$

Whereas Morel and Bricaud (1981) assumed a constant value of a_{cm} ($= 2 \times 10^5$ m^{-1}) at the blue peak for calculation of Q_a, we found that values varied from 1.1 to 2.3 $\times 10^5$ m^{-1} mainly due to changes in c. At the red absorption peak, values were as low as 0.4×10^5 m^{-1} due to the decreased Chl *a*-specific absorption at red wavelengths compared to blue and the lack of absorption by accessory pigments at red wavelengths.

Morel and Bricaud (1981) have described absorption efficiency as a theoretical function of the dimensionless parameter, $\rho'(\lambda)$. This parameter represents the optical thickness of a particle along its diameter and is defined as

$$\rho'(\lambda) = a_{cm}(\lambda)\, d \qquad (2)$$

where d is the particle diameter. The absorption efficiency, $Q_a(\lambda)$, is the fraction of the photons incident on the geometric cross-section of the cell that is absorbed by the cell. From the absorption coefficient for phytoplankton in a suspension $a_{ph}(\lambda)$, $Q_a(\lambda)$ can be calculated as

$$Q_a(\lambda) = \frac{a_{ph}(\lambda)\, V}{(\pi d^2/4)\, N}. \qquad (3)$$

Here N is the number of cells in a volume V of the suspension, and cells are assumed to be spherical and homogenous (Morel and Bricaud 1981). The measurements that we have made allow independent calculations of both $\rho'(\lambda)$ and $Q_a(\lambda)$ for *D. tertiolecta* at each μ (Fig. 3). An index of the package effect, $Q_a^*(\lambda)$, which is the ratio of absorption by discrete packages to the absorption by the same material dispersed in solution, has also been presented by Morel and Bricaud (1981):

$$Q_a^*(\lambda) = a_{ph}^*(\lambda)/a_{sol}^*(\lambda). \qquad (4)$$

We applied this equation with $a_{TX}^*(\lambda)$ for $a_{sol}^*(\lambda)$ in order to calculate values of $Q_a^*(\lambda)$. For these growth conditions and wavelengths, Q_a ranges from 0.2 to nearly 0.6, while Q_a^* varies from almost 0.9 to as low as 0.5 and agreement with theory is excellent (Fig. 3). This variability suggests that less severely N-limited cells can absorb more light and thus grow more rapidly. This increase in overall absorption by the cell is accompanied, however, by a decrease in the

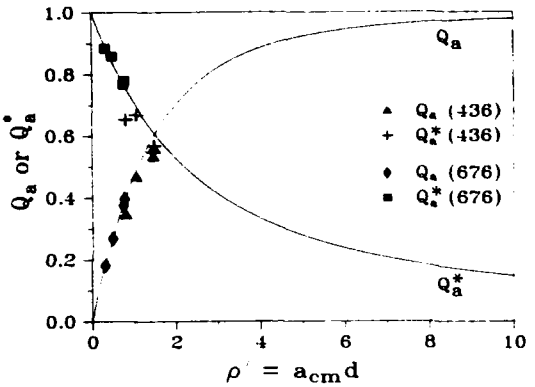

Fig. 3. In vivo absorption efficiency (Q_a) and the packaging parameter (Q_a^*) at the red and blue absorption peaks as a function of cellular optical thickness (ρ') for each of the growth conditions examined. Q_a, Q_a^*, and ρ' are estimated from measurements with Eq. 1–4 as described in the text; the theoretical relationships of Morel and Bricaud (1981) are shown for comparison (solid lines).

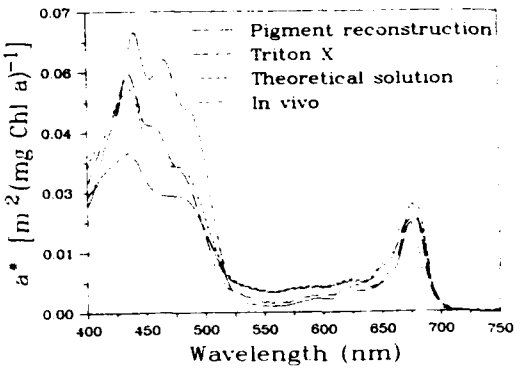

Fig. 4. A comparison of several methods for estimating unpackaged Chl-*a*-specific absorption for *Dunaliella tertiolecta* grown at 0.61 d^{-1}. Absorption by cells solubilized in Triton X is similar to that calculated for a theoretical solution of cell material, but the pigment reconstruction technique significantly overestimates unpackaged absoprtion (details of these methods given in text). The magnitude of in vivo absorption, which includes the manifestation of package effects, is shown for comparison. These results are typical of all the growth rates.

efficiency with which each molecule of pigment absorbs.

Pigment reconstruction of absorption—Because of the need for accurate estimates of $a_{ph}^*(\lambda)$ in bio-optical models, a great deal of effort is currently being focused on the determination of this parameter for natural samples. Because other absorbing particles are present in these samples, direct measurements of particulate absorption are not sufficient to specify $a_{ph}^*(\lambda)$. This problem has led to the development of alternative methods for deriving $a_{ph}^*(\lambda)$, including reconstruction of $a_{ph}^*(\lambda)$ from HPLC data on individual pigment abundances (Bidigare et al. 1987). By summing the contributions of each of the individual pigments, $a_{ph}^*(\lambda)$ can be estimated:

$$a_{ph}^*(\lambda) = \sum a_i^*(\lambda)\, C_i/\text{Chl } a. \qquad (5)$$

Here $a_i^*(\lambda)$ is the specific absorption coefficient of pigment i at wavelength λ, C_i the concentration of pigment i in the suspension, and Chl a the concentration of Chl a in the suspension.

We have made this calculation for each of the growth conditions studied using the spectral specific absorption coefficients for Chl *a*, Chl *b*, and photoprotective carotenoids from Bidigare et al. (1990). Because these coefficients are derived from absorption of individual pigments in solvents, any in vivo package effects will not be reflected in $a_{ph}^*(\lambda)$ estimated from Eq. 5. For this reason we expect this estimate of $a_{ph}^*(\lambda)$ to be comparable to the measured $a_{TX}^*(\lambda)$. In the blue-to-green region of the spectrum, reconstructed $a_{ph}^*(\lambda)$ values are up to 2.5 times the true $a_{ph}^*(\lambda)$ and as much as 2 times $a_{TX}^*(\lambda)$, with the largest differences at the highest growth rates (Fig. 4 shows results at $\mu = 0.61$ d^{-1}). For the various growth rates, the mean value from 400 to 500 nm of the reconstructed $a_{ph}^*(\lambda)$ ranges from 23 to 31% higher than $a_{TX}^*(\lambda)$.

As an additional comparison, we have also calculated the theoretical absorption in solution [$a_{sol}^*(\lambda)$] following the method of Morel and Bricaud (1981). Inputs to this calculation are the measured in vivo absorption and the cell diameter, with the theory then allowing extrapolation to absorption at zero particle diameter (i.e. for the same material in solution). For the average absorption from 400 to 500 nm, $a_{sol}^*(\lambda)$ is consistently lower than the measured $a_{TX}^*(\lambda)$, but in contrast to the reconstructed estimate the difference ranges from 2% to at most 13%.

The highest values of $a_{ph}^*(\lambda)$ we estimated

with the pigment reconstruction technique correspond to values of $Q_a(\lambda)$ that are higher than the theoretical maximum of 1. Undoubtedly package effects must be included before this method can provide realistic estimates. The reason for the discrepancy between $a_{TX}^*(\lambda)$ and the estimate of $a_{ph}^*(\lambda)$ from pigment reconstruction, however, remains elusive. The overestimate seems to be due mainly to the contribution of lutein, although the other carotenoids also play a role. It is possible that the magnitude of absorption by these carotenoids in vivo is significantly different than in organic solvents due to more than package effects. Recent application of the pigment reconstruction technique in a dinoflagellate includes a correction for package effects (Nelson and Prézelin 1990), but our observations suggest that even this modification would not give accurate results for *D. tertiolecta*. We speculate that the molar extinction coefficient for some of these pigments in organic solvents is greater than the corresponding coefficient for the same pigment in theoretical aqueous solution. Whether this type of problem exists for other taxa with different pigmentation must be tested with further study of laboratory cultures.

Fluorescence changes—Fluorescence from a single cell has been described by a theoretical model that incorporates the role of pigment packaging in modifying light absorption efficiency and intracellular reabsorption of fluorescence (Collins et al. 1985; Mitchell and Kiefer 1988). This model can be applied to conditions of broadband excitation and emission and can be modified to estimate the relative fluorescence measured by a specific detector, thus allowing the model to be evaluated with our data set. Collins et al. (1985) presented a functional form for fluorescence emission from a cell which is generalized here to reflect the effects of both excitation and emission wavelengths:

$$F(\lambda_e, \lambda_f) = \phi_f(\lambda_e, \lambda_f)\, E(\lambda_e)\, Q_a(\lambda_e) \cdot (\pi d^2/4)\, Q_a^*(\lambda_f). \quad (6)$$

Here ϕ_f is the quantum yield for fluorescence, E is the incident irradiance, and λ_e and λ_f are the excitation and emission wavelengths. This generalized equation should be applicable in cases where multiple chromaphores with different quantum yields such as chlorophyll and phycoerythrin may be contributing to the fluoresced light and is valid for both excitation and emission spectra. It is also possible to express fluorescence in terms of $a_{ph}^*(\lambda_e)$, $a_{ph}^*(\lambda_f)$, and $a_{cm}(\lambda_f)$ if the available information is not sufficient to determine absorption efficiencies (Mitchell and Kiefer 1988).

For spectrally specified excitation irradiance and absorption properties, $Q_a(\lambda)$ and $Q_a^*(\lambda)$, Eq. 6 can be integrated over the ranges of λ_e and λ_f to give the total flux of fluoresced quanta in a broad emission band as a result of polychromatic excitation. In order to calculate the flourescence from a single cell measured by a specific instrument, it is necessary to scale the total flux to include the detection characteristics $D(\lambda_f)$ and the geometric constant G that indicates the fraction of the emitted light intercepted by the detector. The resulting expression is

$$\bar{F} = G \int_{\lambda_f} \int_{\lambda_e} D(\lambda_f)\, F(\lambda_e, \lambda_f)\, d\lambda_e\, d\lambda_f \quad (7)$$

where $\bar{F}$ is the fluorescence from a single cell for broadband excitation and emission, and $F(\lambda_e, \lambda_f)$ is as defined in Eq. 6 with $E(\lambda_e)$ the product of the spectral irradiance emitted by the excitation source and the transmission properties of any filters or optical components between the source and the sample. Similarly, the detection function $D(\lambda_f)$ is the product of the transmission of any emission filters or optical components and the response of the detector at each wavelength λ_f. This fluorescence can also be expressed per unit of Chl as $\bar{F}^*$ which is simply $\bar{F}$ divided by the cellular concentration of Chl *a*.

Consistent with the foregoing theory, variability with growth rate documented for specific absorption is also evident in the fluorescence data. Despite differences in spectral characteristics, results for the Sea Tech fluorometer (Table 2) and trends observed with the Turner Designs fluorometer were similar. For comparison of trends, all fluorescence data have been expressed in rel-

Table 2. Quantum yield for growth and optical properties of N-limited *Dunaliella tertiolecta*. Quantum yield has units of mol C (mol quanta)$^{-1}$; specific absorption coefficients are given for the red and blue peaks in m^2 (mg Chl *a*)$^{-1}$; absorption efficiencies are dimensionless and fluorescence is expressed as relative flux per cell ($\bar{F}$) or per unit of Chl *a* ($\bar{F}^*$).

	Growth rate (d^{-1})			
	0.23	0.61	1.05	2.08
$\phi\mu$	0.013	0.021	0.027	0.048
$a_{ph}^*(436)$	0.040	0.037	0.025	0.027
$a_{ph}^*(676)$	0.021	0.022	0.018	0.019
$a_{TY}^*(435)$	0.061	0.056	0.044	0.049
$a_{TY}^*(668)$	0.024	0.025	0.023	0.025
$Q_a(436)$	0.35	0.47	0.56	0.54
$Q_a(676)$	0.18	0.27	0.40	0.38
$Q_a^*(436)$	0.66	0.67	0.57	0.55
$Q_a^*(676)$	0.88	0.86	0.78	0.77
Sea Tech fluorometer				
Measured				
$\bar{F}$	1.00	1.50	1.20	1.40
$\bar{F}^*$	1.00	1.04	0.53	0.60
Modeled				
$\bar{F}$	1.00	1.35	1.32	1.54
$\bar{F}^*$	1.00	0.94	0.59	0.66

ative numbers scaled to be 1 at the lowest μ. At the highest μ, although pigment per cell more than doubled relative to the lowest μ, Q_a is higher by only 60% at the blue peak and a correspondingly small increase is observed in $\bar{F}$. As pigment per cell increases, changes in the pigment composition and in the severity of package effects are acting as described above to decrease $a_{ph}^*(\lambda)$.

A similar decline in $\bar{F}^*$ is also evident. Because cell suspensions were kept optically thin [OD(675) $\leq$ 0.01] for all fluorescence measurements, reabsorption of fluoresced light within the suspension cannot account for the observed variability in fluorescence. For the Turner Designs measurements, red absorption by the cells in suspension was about equal to absorption by the water medium and an order of magnitude lower than absorption by the water for measurements with the Sea Tech fluorometer. Although it is possible that variability in the quantum yield of fluorescence (number of photons fluoresced per number absorbed) could occur for cells from different growth conditions, the trends we observed suggest that variability in the efficiency with which light is absorbed is an important factor.

From observed values of absorption and cell size and the known characteristics of the Sea Tech fluorometer, we have also predicted the relative fluorescence with Eq. 6 and 7. Because we do not have information concerning variability in ϕ_f, as a first approximation we have assumed that it is constant for the excitation and emission conditions used and that it does not vary over the growth conditions examined. Because we do not know the absolute values of ϕ_f and G, fluorescence values have been presented as relative numbers scaled to maximum of 1 at μ of 0.23 d^{-1}. As indicated above, these calculations involve not only spectral values of the absorption factors for the cells but also the spectral output of the lamp and the spectral transmission of the blue excitation filter, the acrylic window, the red emission filter, and the gold mirror, as well as the spectral sensitivity of the detector (*see* Bartz et al. 1988).

Trends in values of $\bar{F}^*$ predicted with Eq. 6 and 7 agree well with actual measurements (Table 2, $r^2 = 0.96$), which supports our hypothesis that changes in absorption efficiency are an important source of variability in fluorescence per Chl *a* and demonstrates the validity of the model for broadband excitation and emission of fluorescence. Regression with the measured and modeled values as independent and dependent variables, respectively, reveals an intercept of 0.20. With so few points it is not reasonable to attach much significance to this intercept, but it is possible that it reflects a change in ϕ_f with growth conditions. Only a larger range of experimental conditions and more detailed work on variability in $\bar{F}^*$ can test this hypothesis. Further, the broadband approach presented here is somewhat crude, and spectral fluorescence methods such as those of Mitchell and Kiefer (1988) will be necessary to resolve the details in model verification.

The variability in fluorescence properties observed must be considered in the context of the increasing use of in situ fluorometers to estimate phytoplankton biomass. Although with proper calibration this method may provide useful information, no simple relationship can be expected to exist between fluorescence and biomass estimates

such as Chl *a* concentration. Both variability with growth conditions for a single species and the potential for interspecific differences must be considered. In addition, the lack of knowledge concerning variability in the quantum yield for fluorescence continues to limit applications such as the use of natural fluorescence to estimate productivity.

Quantum yield for growth—The quantum yield at the irradiance under which cells have been grown, ϕ_μ, can be determined from a spectral version of the model of Kiefer and Mitchell (1983):

$$\mu = \phi_\mu \, \text{Chl:C} \int_\lambda a_{ph}^*(\lambda) \, E_0(\lambda) \, d\lambda. \quad (8)$$

Here μ is the specific growth rate of the cells, $E_0(\lambda)$ is the spectral growth irradiance, and Chl : C is the cellular Chl *a* : C ratio. Solving this equation for ϕ_μ at each of the growth rates examined results in nearly fourfold variability in ϕ_μ, with values decreasing as N limitation increases (Table 2).

A potential source of variability in ϕ_μ or ϕ_{ph} is changes in $a_{ph}^*(\lambda)$ due to pigment-ratio shifts. If the abundance of photoprotective pigments increases relative to photosynthetic pigments, $a_{ph}^*(\lambda)$ is expected to increase but the energy available for C fixation would decrease. The result is a decrease in ϕ_μ with higher $a_{ph}^*(\lambda)$, consistent with our observations of increased abundance of lutein and β-carotene relative to Chl *a* at low μ. This increase in $a_{ph}^*(\lambda)$ can only account for ~25% of the change we oberved in ϕ_μ, however, because ϕ_μ varied by more than threefold and pigment-ratio-induced changes in $a_{ph}^*(\lambda)$ were much smaller (*see Table 2*).

Many factors besides $a_{ph}^*(\lambda)$ may contribute to a decrease in ϕ_μ, including changes in respiration relative to photosynthesis with growth rate. Although we have not measured respiration in this study, it is unlikely that increased respiration relative to growth could account for all of the decrease in ϕ_μ observed at low μ. For N-limited growth of *Pavlova lutheri*, Chalup and Laws (1990) found a more than twofold increase in ϕ_{ph} with μ and also demonstrated an increase in ϕ_{ph} with decreased irradiance at the same dilution rate. For N limitation of *Isochrysis galbana* at a single irradiance, Herzig and Falkowski (1989) observed a range in ϕ_μ similar to our observations and additionally found that variability in ϕ_{ph} was 85% of that for ϕ_μ.

Additional sources of variability in quantum yield were not investigated in this study. Changes in energy transfer efficiency, in the reaction center turnover time, or in the abundance of pigment in photosystem 1 relative to photosystem 2 could all contribute to changes in ϕ_μ. Although Cleveland and Perry (1987) have implicated these mechanisms to explain quantum yield changes in transition from nutrient-replete to nutrient-starved conditions, results may differ for cultures allowed to adapt to a steady state N-limited growth condition. Using pump and probe fluorescence techniques and immunochemistry, Kolber et al. (1988) suggested that N limitation in several species, including *D. tertiolecta*, leads to a decrease in the energy conversion efficiency of photosystem 2 caused by a loss of functional reaction centers or inefficient energy transfer to the reaction centers.

All of these results suggest that studies considering photosynthetic efficiency as independent of nutrient availability must be viewed with caution. Kiefer and Mitchell (1983) hypothesized that ϕ_{ph} is a function only of irradiance, consistent with their model for growth of *Thalassiosira fluviatilis* in which spectrally averaged a_{ph}^* was assumed to be constant. Sakshaug et al. (1989) used a similar fitting technique to model growth rate under a large number of light- and nutrient-limited conditions and found a constant value of the product $a_{ph}^* \cdot \phi_{ph}$ to be adequate for a given irradiance. The conclusion that ϕ_{ph} is only a function of growth irradiance alone and not of nutrient limitation, however, has not been substantiated by studies in which light absorption and photosynthetic efficiency have been measured (e.g. this study; Kolber et al. 1988; Herzig and Falkowski 1989).

Conclusion

It is evident that variability in the physiological responses of phytoplankton to growth conditions cannot be ignored in bio-optical characterization of ocean waters both

with respect to productivity and optical properties. Models for the remote estimation of pigments or for propagation of light through the water column rely on accurate knowledge of the relationships between pigments and in situ optical properties. For example, recent work suggests that predictions with current algorithms for pigment estimation may lead to significant errors for the Antarctic Ocean (Mitchell and Holm-Hansen 1991). These errors result from variability in $a_{ph}^*(\lambda)$ and in the relative abundance of phytoplankton and other absorbing material in the water column. Estimating photosynthetic biomass from in situ fluorescence measurements is equally complex and can be significantly affected by the physiological state of the phytoplankton.

Bio-optical models of phytoplankton growth and productivity must also incorporate physiological variability if light absorption is to be accurately related to C fixation. Working with a model similar to that of Kiefer and Mitchell (1983), Sakshaug et al. (1989) found that, compared to other model parameters, changes in the value of a_{ph}^* caused relatively large errors in modeled growth rate. Increasing evidence of large variability in the optical properties of phytoplankton with growth conditions suggests that modification of existing models to incorporate physiology and environmental conditions besides light intensity must be a high priority. A major obstacle to the achievement of this goal continues to be a lack of comprehensive physiological studies that include simultaneous measurement of pigments and optical properties for a wide range of species and growth conditions.

References

BANNISTER, T. T. 1979. Quantitative description of steady state, nutrient-saturated algal growth, including adaptation. Limnol. Oceanogr. **24:** 76–96.

BARTZ, R., R. W. SPINRAD, AND J. C. KITCHEN. 1988. A low power, high resolution, in situ fluorometer for profiling and moored applications in water, p. 157–170. *In* Ocean Optics 9, Proc. SPIE **925.**

BERNER, T., K. WYMAN, AND P. G. FALKOWSKI. 1989. Photoadaptation and the package effect in *Dunaliella tertiolecta* (Chlorophyceae). J. Phycol. **25:** 70–78.

BIDIGARE, R. R. 1989. Photosynthetic pigment composition of the brown tide alga: Unique chlorophyll and carotenoid derivatives, p. 57–75. *In* E. M. Cosper et al. [eds.], Coastal and estuarine studies. Springer.

———, M. E. ONDRUSEK, J. H. MORROW, AND D. KIEFER. 1990. In vivo absorption properties of algal pigments, p. 290–302. *In* Ocean Optics 10, Proc. SPIE **1302.**

———, R. C. SMITH, K. S. BAKER, AND J. MARRA. 1987. Oceanic primary production estimates from measurements of spectral irradiance and pigment concentrations. Global Biogeochem. Cycles **1:** 171–186.

BRICAUD, A., A. L. BEDHOMME, AND A. MOREL. 1988. Optical properties of diverse phytoplanktonic species: Experimental results and theoretical interpretation. J. Plankton Res. **10:** 851–873.

———, A. MOREL, AND L. PRIEUR. 1983. Optical efficiency factors of some phytoplankters. Limnol. Oceanogr. **28:** 816–832.

CAPERON, J., AND J. MEYER. 1972. Nitrogen-limited growth of marine phytoplankton-1. Changes in population characteristics with steady-state growth rate. Deep-Sea Res. **19:** 601–618.

CHALUP, M. S., AND E. A. LAWS. 1990. A test of the assumptions and predictions of recent microalgal growth models with the marine phytoplankter *Pavlova lutheri*. Limnol. Oceanogr. **35:** 583–596.

CLEVELAND, J. S., AND M. J. PERRY. 1987. Quantum yield, relative specific absorption and fluorescence in nitrogen-limited *Chaetoceros gracilis*. Mar. Biol. **94:** 489–497.

COLLINS, D. J., D. A. KIEFER, J. B. SOOHOO, AND I. S. MCDERMID. 1985. The role of reabsorption in the spectral distribution of phytoplankton fluorescence emission. Deep-Sea Res. **32:** 983–1003.

DUYSENS, L. N. M. 1956. The flattening of the absorption spectrum of suspensions, as compared to that of solutions. Biochim. Biophys. Acta **19:** 1–12.

FALKOWSKI, P. G., Z. DUBINSKY, AND K. WYMAN. 1985. Growth-irradiance relationships in phytoplankton. Limnol. Oceanogr. **30:** 311–321.

HERZIG, R., AND P. G. FALKOWSKI. 1989. Nitrogen limitation in *Isochrysis galbana* (Haptophyceae). 1. Photosynthetic energy conversion and growth efficiency. J. Phycol. **25:** 462–471.

KIEFER, D. A. 1973. Chlorophyll *a* fluorescence in marine centric diatoms: Responses of chloroplasts to light and nutrient stress. Mar. Biol. **23:** 39–46.

———, AND B. G. MITCHELL. 1983. A simple steady state description of phytoplankton growth based on absorption cross section and quantum efficiency. Limnol. Oceanogr. **28:** 770–776.

KOLBER, Z., J. ZEHR, AND P. G. FALKOWSKI. 1988. Effects of growth irradiance and nitrogen limitation on photosynthetic energy conversion in photosystem 2. Plant Physiol. **88:** 923–929.

LOEBLICH, A. R., III. 1975. A seawater medium for dinoflagellates and the nutrition of *Cachonina niei*. J. Phycol. **11:** 80–86.

MITCHELL, B. G., AND O. HOLM-HANSEN. 1991. Bio-optical properties of Antarctic waters: Differentiation from temperate ocean models. Deep-Sea Res. **38:** 1009–1028.

———, AND D. A. KIEFER. 1988. Chlorophyll *a* spe-

cific absorption and fluorescence excitation spectra for light-limited phytoplankton. Deep-Sea Res. **35:** 639–663.

MOREL, A. 1988. Optical modeling of the upper ocean in relation to its biogenous matter content (case I waters). J. Geophys. Res. **93:** 10.749–10.768.

———, AND A. BRICAUD. 1981. Theoretical results concerning light absorption in a discrete medium, and applications to specific absorption of phytoplankton. Deep-Sea Res. **28:** 1375–1393.

NELSON, N. B., AND B. B. PRÉZELIN. 1990. Chromatic light effects and physiological modeling of absorption properties of *Heterocapsa pygmaea* (= *Glenodimium* sp.). Mar. Ecol. Prog. Ser. **63:** 37–46.

SAKSHAUG, E., K. ANDRESEN, AND D. A. KIEFER. 1989. A steady state description of growth and light absorption in the marine planktonic diatom *Skeletonema costatum*. Limnol. Oceanogr. **34:** 198–205.

SATHYENDRANATH, S., L. LAZZARA, AND L. PRIEUR. 1987. Variations in the spectral values of specific absorption of phytoplankton. Limnol. Oceanogr. **32:** 403–415.

SHIBATA, K. 1958. Spectroscopy of intact biological materials. Absolute and relative measurements of their transmission, reflection and absorption spectra. J. Biochem. **45:** 599–623.

SMITH, R. C., B. B. PRÉZELIN, R. R. BIDIGARE, AND K. S. BAKER. 1989. Bio-optical modeling of photosynthetic production in coastal waters. Limnol. Oceanogr. **34:** 1524–1544.

SOSIK, H. M., S. W. CHISHOLM, AND R. J. OLSON. 1989. Chlorophyll fluorescence from single cells: Interpretation of flow cytometric signals. Limnol. Oceanogr. **34:** 1749–1761.

WELSCHMEYER, N. A., AND C. J. LORENZEN. 1981. Chlorophyll-specific photosynthesis and quantum efficiency at subsaturating light intensities. J. Phycol. **17:** 283–293.

Submitted: 12 September 1990
Accepted: 22 January 1991
Revised: 28 May 1991

PROCEEDINGS REPRINT

SPIE—The International Society for Optical Engineering

Reprinted from

Ocean Optics X

16-18 April 1990
Orlando, Florida

Volume 1302

Algorithms for Determining the Absorption Coefficient of Aquatic Particulates Using the Quantitative Filter Technique (QFT)

B. Greg Mitchell
Marine Research Division, A-018
Scripps Institution of Oceanography
University of California, San Diego
La Jolla, California 92093

ABSTRACT

Particulates in aquatic environments dominate variability in inherent and apparent optical properties. Dilute concentrations have made the quantitative determination of particulate absorption a relatively difficult problem. A quantitative filter technique (QFT) has been described previously[1,2] which allows determination of the particulate absorption coefficient ($a_p(\lambda)$) for samples concentrated on filters by correcting for the pathlength amplification effect (β). Details of the generality, accuracy and precision of the procedure have not been reported previously.

A spectrophotometer equipped with an integrating sphere accessory was used to study the optical density of phytoplankton suspensions and colored polystyrene beads, $OD_s(\lambda)$, and the optical density of the same suspensions on a variety of common filter types, $OD_f(\lambda)$. The ratio of $OD_f(\lambda)/OD_s(\lambda)$ confirms that multiple scattering in filters leads to variable β, a non-linear function of $OD_f(\lambda)$. Studies of $OD_f(\lambda)$ when the filters are mounted in different positions in a single spectrophotometer, and for standard and integrating sphere spectophotometers indicate that the procedures presented are of general applicability. With proper care in baseline correction and sample preparation, spectra of $a_p(\lambda)$ can be calculated from measurements of $OD_f(\lambda)$ for aquatic particles of diverse size and refractive index with an accuracy of better than ± 15%. A comparison of filter types commonly used for aquatic research indicates that different algorithms are required for estimation of $a_p(\lambda)$ from $OD_f(\lambda)$ measurements using different filter types.

1. INTRODUCTION

The spectral absorption coefficient ($a(\lambda)$) is an inherent optical property of aquatic systems[3,4]. As an inherent optical property, $a(\lambda)$ can be partitioned into its subcomponents:

$$a(\lambda) = a_w(\lambda) + a_s(\lambda) + a_p(\lambda) \quad (1)$$

where a_w, a_s and a_p are the portion of the coefficient attributable to water, soluble constituents and particulates, respectively.

Variations in the apparent optical properties of water, including the spectral diffuse attenuation coefficient $k(\lambda)$ and irradiance reflectance $R(\lambda)$, are determined by variations in the spectral backscatter coefficient $b_b(\lambda)$ and $a(\lambda)$[3-5]:

$$k(\lambda) \simeq D\, a(\lambda) + b_b(\lambda) \tag{2}$$

$$R(\lambda) \simeq 0.33\, b_b(\lambda) / a(\lambda) \tag{3}$$

where D is the radiance distribution function. Thus, understanding variability in $a(\lambda)$ is crucial for understanding variability in these (and other) apparent optical properties of aquatic systems. Since $a_p(\lambda)$ dominates the variability of $a(\lambda)$ in oceanic waters with little terrestrial influence, it is among the most important parameters which must be measured for a complete description of the optical properties of aquatic systems.

The method of concentrating marine particles on filters for measurement of optical density ($OD_f(\lambda)$) was originally applied in field studies nearly thirty years ago by Charles Yentsch[6]. $OD_f(\lambda)$ is calculated from the ratio of the transmittance through a reference, $T_r(\lambda)$, and sample filter, $T_s(\lambda)$:

$$OD_f(\lambda) = -\mathrm{Log}_{10}\,(T_s(\lambda)/T_r(\lambda)) \tag{4}$$

Kiefer and Soo Hoo[7] demonstrated that the observed magnitude of $OD_f(\lambda)$ was greater than one would predict based on the geometric pathlength of the ratio of volume filtered (V_f) to clearance area of the filter (A_c). They concluded that the optical pathlength was greater than the geometric pathlength due to scattering by the filter. Butler[8] defined the phenomenon of pathlength amplification for absorption of material in scattering suspensions:

$$\beta = l_o / l_g \tag{5}$$

where l_o and l_g are the optical and geometric pathlengths, respectively. The value of l_g for particles concentrated on filters is simply the ratio of the volume filtered to the clearance area of the filter:

$$l_g = V_f / A_c \tag{6}$$

where

$$A_c = \pi r^2 \tag{7}$$

and where r is the radius of the portion of the filter which contains the particles removed from the suspension. From the above relationships, the absorption coefficient $a_p(\lambda)$ can be calculated:

$$a_p(\lambda) = 2.3\, OD_f(\lambda) / (l_g\, \beta) \tag{8}$$

The factor 2.3 converts Log_{10} to Log_e.

Mitchell and Kiefer[1,2] demonstrated the non-linear relationship between β and $OD_f(\lambda)$, and suggested that simple empirical relationships could be used to make quantitative estimates of $a_p(\lambda)$ from measurements of $OD_f(\lambda)$. The concept of this quantitative filter technique (QFT) for correction of β to estimate $a_p(\lambda)$ for dilute suspensions has been widely applied[1,2,7,9-13] but there has been little uniformity with respect to correction methodology. A review of inconsistencies in methods presented in the literature indicates that the various methods might differ by as much as two-fold in the final estimate of $a_p(\lambda)$. For example, Kiefer and Soo Hoo[7] based their estimates of β on a comparison between $OD_f(\lambda)$ determined on field samples and diffuse absorption coefficients determined for

cultures[14]. Subsequently, others have used the same β for estimates of the absorption coefficient which may be as small as half the value of the diffuse absorption coefficient[3]. An evaluation of the QFT methodology, its generality, precision and accuracy is presented in this report.

2. METHODS

Cultures of unicellular algae were grown in nutrient enriched media and the optical density of suspensions ($OD_s(\lambda)$) was measured in a spectrophotometer. A variety of cell sizes and taxonomic types were used including chlorophytes (*Dunaliella tertiolecta*; *Chlorella sp.*; *Nanochloroxis sp.*); a bacillariophyte (*Thalasiossira fluviatilis*); and a cyanobacterium (*Synechococus sp.*). Cell sizes ranged from 2-20 μm. Blue polystyrene beads (2.85 μm, Polysciences, Inc.) were also used as a particle type with high refractive index relative to water ($n \simeq 1.2$), compared to the algae ($n \simeq 1.05$-1.1). The refractive index of polystyrene is approximately 1.45 relative to air. In addition, a sample of natural sea water collected from the Scripps Institution of Oceanography pier was concentrated by filtration and resuspended for measurement of $OD_s(\lambda)$ according to the methods of Kirk[15].

Measurements of $OD(\lambda)$ were made with a dual grating double beam Perkin-Elmer Lambda 6 spectrophotometer equipped with an integrating sphere. Data acquisition was accomplished via a digital IEEE 488 interface between the spectrophotometer and a personal computer. The spectrophotometer automatically corrected for the baseline which was stored prior to analyses of different types. For suspensions, the baseline was a filtrate of the growth medium. For the beads, distilled water was used. For the filters, the baseline was determined for filters which were saturated with the filtrate of the growth medium or distilled water, in the case of analysis of beads. Values of $OD_s(\lambda)$ were directly determined for suspensions of cells or beads using the integrating sphere attachment with the appropriate medium in the reference beam. For phytoplankton and natural particulates from sea water, spectra were set to 0.0 at 750 nm. The suspensions were concentrated onto various filter types for determination of $OD_f(\lambda)$, with the appropriate filter type in the reference beam. The reference and sample filter were kept saturated during the analyses. This was ensured by cutting a section of 1 cm width from the center of the filter, and placing the section into a 1 cm cuvette with a drop of the appropriate fluid. Caution must be exercised to maintain saturation, but not oversaturation which can result in resuspension of particles off the filter. Filter types studied included Whatman glass fiber types GF/F, GF/C, 934AH and Millepore cellulose acetate type HA.

The relationships between $OD_s(\lambda)$ and $OD_f(\lambda)$ were studied using statistical curve fitting procedures in SYSTAT, a commercial software package available for personal computers. Various procedures to fit the observed non-linearity in the relationship between $OD_s(\lambda)$ and $OD_f(\lambda)$ were investigated, and a simple quadratic equation (second order polynomial) was found to be the most satisfactory. Thus, the magnitude of $OD_s(\lambda)$ may be estimated directly from $OD_f(\lambda)$ by a relationship of the form:

$$OD_s(\lambda) = a\, OD_f(\lambda) + b\, [OD_f(\lambda)]^2 \qquad (9)$$

2. RESULTS AND DISCUSSION

2.1 Generality of $OD_f(\lambda)$ determinations

Of paramount concern with respect to the utilization of the QFT is the issue of the generality of determination of $OD_f(\lambda)$ using different spectrophotometers or different optical geometry for determining $T_r(\lambda)$ and $T_s(\lambda)$. Provided that the post-sample path length for the reference and sample positions is equivalent, the primary difference between systems or configurations is the angle of acceptance of the scattered light transmitted from the diffusing sample to the detector. Changing the angle of acceptance from the sample to the detector could hypothetically cause variations in the $OD_f(\lambda)$ observed for the same sample.

An experiment was done to evaluate the effects of varying acceptance angle of the post-sample beam. $OD_f(\lambda)$ was determined for 3 separate positions along the optical axis in the sample compartment of the Lambda 6 spectrophotometer configured without the integrating sphere. A fourth geometry, attained by determining $OD_f(\lambda)$ using the integrating sphere, resulted in an angle of acceptance of nearly 180°. For each geometry, a baseline was determined by placing blank filters in the sample and reference positions. $OD_f(\lambda)$ was then determined for replicate samples which had the same volume of a culture of *D. tertiolecta* filtered onto GF/F filters. Results of this experiment are presented in Figure 1. There was no significant difference between values of $OD_f(\lambda)$ for the different positions, or for the integrating sphere determination. Differences between replicate samples was comparable to differences for the various measurement geometries.

2.2 Detailed studies of GF/F and GF/C filter types

The most commonly used filters for either oceanographic field work or laboratory work are of the Whatman GF/F or GF/C type. Among the concerns raised by other investigators regarding the

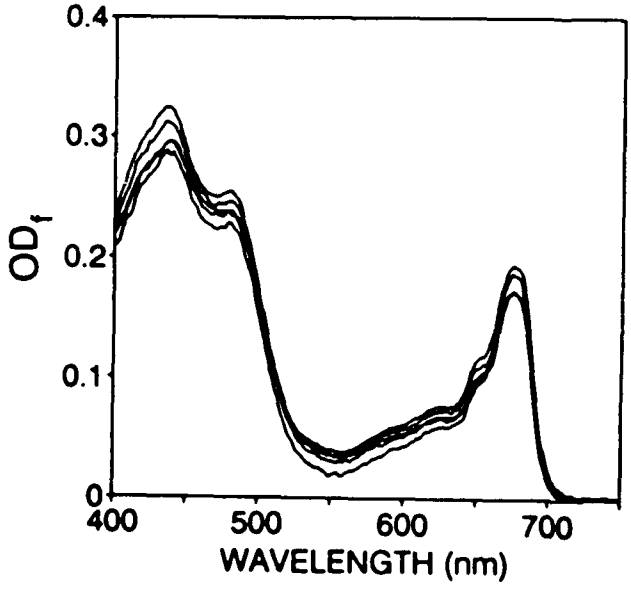

Figure 1. A comparison of observations of $OD_f(\lambda)$ for different optical geometries. After storing a baseline for each sample position, $OD_f(\lambda)$ was determined for duplicate filters containing the same volume filtered of *D. tertiolecta*. Samples were placed along the optical axis at the front, center and back of the sample compartment (15 cm range) and in the integrating sphere attachment. Each curve is the mean of the duplicate samples for each position. Difference between duplicates was comparable to the overall difference observed, suggesting that post-sample optical geometry is not a significant problem for the general application of the QFT.

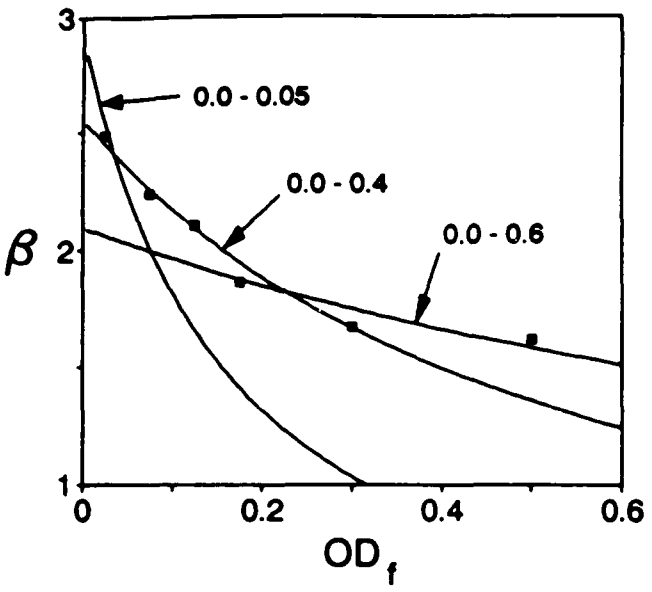

Figure 2. Analysis of the relationship between β and $OD_f(\lambda)$ for quadratic equation curve fits including different subsets of the total data base for GF/F filters. Exclusion of high $OD_f(\lambda)$ values resulted in a steeper relationship, while inclusion of all data up to $OD_f(\lambda) = 0.6$ caused the relationship to be quite flat. An analysis of the mean β determined for discrete ranges is included as the discrete points in the figure where $\beta = OD_f(\lambda) / OD_s(\lambda)$. The ranges for discrete analyses included $OD_f(\lambda)$ from 0.0-0.05; 0.05-0.1; 0.1-0.15; 0.15-0.2, 0.2-0.4; and 0.4-0.6. The points are plotted in the middle of the range. The curve fit including data in the range 0.0-0.4 best fit the discrete analysis.

QFT was the precision of the technique for different sized particles, or for particles of different refractive index. Although it has been hypothesized[1,2] that the scattering by the filter itself is so intense that variations in particle size or refractive index would cause insignificant differences, this was not previously tested.

A detailed study of the QFT for GF/F and GF/C filters was undertaken with a variety of phytoplankton from different taxonomic groups and of different cell sizes. The phytoplankton used in the analysis included *Dunaliella tertiolecta*, *Chlorella sp.*, *Nanochloroxis sp.*, *Thalassiosira fluviatilis* and a unicellular cyanobacterium *Synechococcus sp.* Among the phytoplankton, the diatom is expected to have the highest refractive index due to the silicate frustule. Polystyrene beads (2.85 μm diameter) were included in the analysis to verify the validity of the approach for high refractive index particles.

A summary of the effects of curve fitting data covering different ranges of OD is illustrated in Figure 2. Values of β as a function of $OD_f(\lambda)$ are presented for curve fits using all GF/F data in the $OD_f(\lambda)$ ranges of 0-0.05; 0-0.4; and 0-0.6. Curve fits using data including higher values of $OD_f(\lambda)$ lead to a flatter response for β due to the lower β at high values of $OD_f(\lambda)$. Thus the low OD region was compromised for a better fit at the high OD end. Conversely, using the limited lower OD range leads to fits which are not adequate for the data at high OD. A separate analysis of β determined from the experimental observations rather than the curve fit is also presented. The discrete points plotted in Figure 2 correspond to the mean value of the ratio of $OD_f(\lambda) / OD_s(\lambda)$ over discrete ranges of $OD_f(\lambda)$, plotted at the center of the range. It is evident that β derived from the curve fit data using the range of 0-0.4 best agrees with the discrete ratio approach up to a maximum OD of 0.4. This is the basis for restricting the final curve fitting to this range. From a practical perspective, one generally does not work with samples with $OD_f(\lambda) > 0.4$. This is particularly true in field situations where particle concentrations are low making it difficult to obtain and filter sufficient water to exceed $OD_f(\lambda)$ of 0.4. Thus restricting the curve fit as done here is expected to yield coefficients of the most general utility.

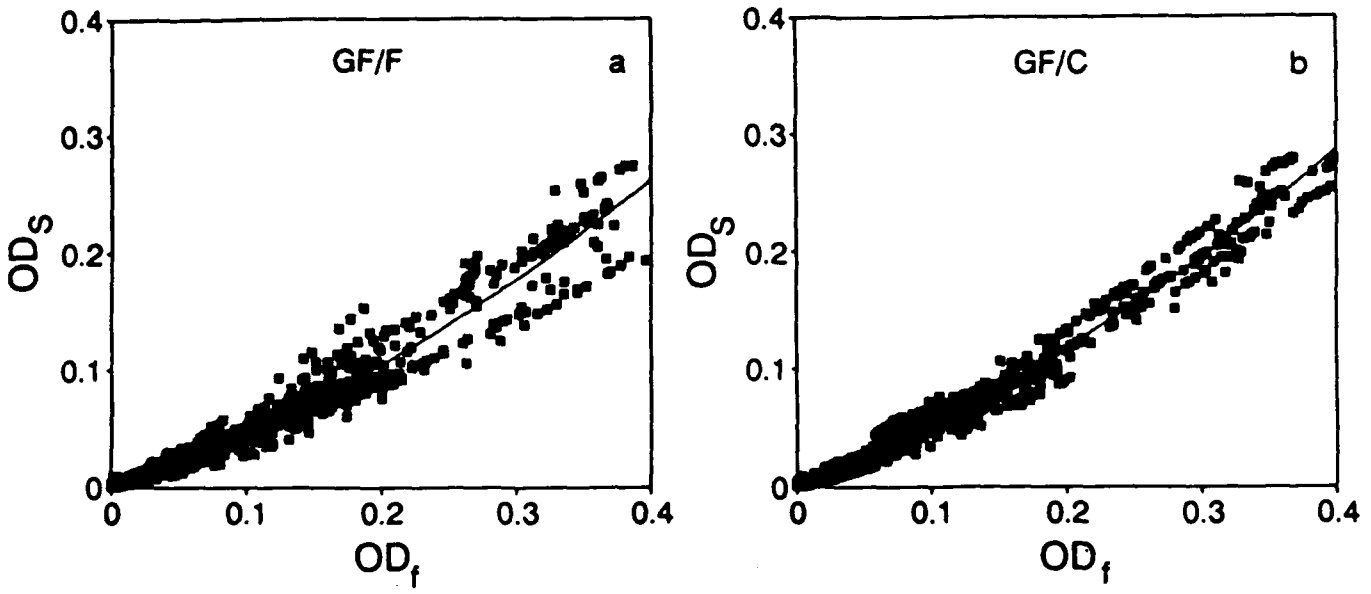

Figure 3. (a) Relationship between $OD_s(\lambda)$ and $OD_f(\lambda)$ for the GF/F filter type and the best fit curve for the range $OD_f(\lambda)$= 0.0-0.4. (b) Relationship between $OD_s(\lambda)$ and $OD_f(\lambda)$ for the GF/C filter type and the best fit curve for the range $OD_f(\lambda)$= 0.0-0.4. Coefficients for the best fit are from Table 1.

		GF/F	GF/C
n observations		6981	5968
a	95% lower	0.380	0.449
	estimate	0.392	0.459
	95% upper	0.404	0.469
b	95% lower	0.610	0.602
	estimate	0.655	0.637
	95% upper	0.700	0.672

Table 1. Coefficients for the quadratic equation fit (Equation 9) of the detailed studies of the relationship between $OD_s(\lambda)$ and $OD_f(\lambda)$ for Whatman GF/C and GF/F filter types. The best estimate and the 95% confidence interval for the coefficients a and b are provided.

Data from this analysis, together with the quadratic equation best fit are presented in Figure 3a (GF/F filter type) and 3b (GF/C filter type). Only data in the range of $OD_f(\lambda)$= 0-0.4 were used in the final curve fitting. Coefficients for the quadratic equation fit, a and b, and the 95% confidence limits for the best fit are provided in Table 1. The best fit results for GF/F and GF/C are presented in Figure 4. Figure 4a illustrates the relationship between $OD_s(\lambda)$ and $OD_f(\lambda)$ for the two filter types, and Figure 4b illustrates the relationship between β and $OD_f(\lambda)$ calculated from the best fit. As reported previously[2], β for GF/F is larger than β for GF/C, and both show a non-linear relationship with $OD_f(\lambda)$ with higher values at low $OD_f(\lambda)$. The upper limit of β using the curve fit method agrees with the upper limit of β = 2.4 specified previously[1,2] as a requirement for optimization of the method so that over-correction did not occur at low values of $OD_f(\lambda)$.

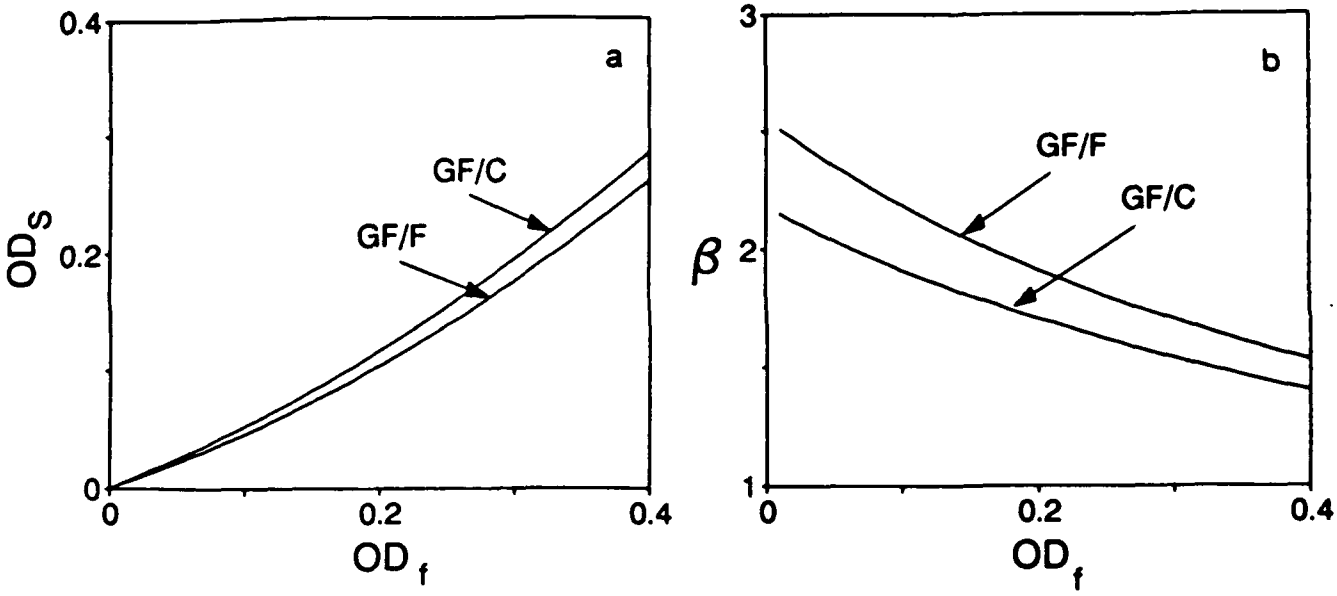

Figure 4. (a) A comparison of the best fit curves for the relationship between $OD_s(\lambda)$ and $OD_f(\lambda)$ for GF/C and GF/F filters (same fit as 3(a) and 3(b). (b) A comparison of the relationship between β, calculated from the best fit in (a), and $OD_f(\lambda)$ for GF/C and GF/F filter types.

2.3 Comparison with previous GF/F algorithm

A significant body of literature exists using the correction procedures outlined in earlier work. The previous procedure for the commonly used GF/F filters was indirect[2,16]: $OD_f(\lambda)$ for the GF/F was converted to the equivalent $OD_f(\lambda)$ for a GF/C, and an optimized β algorithm for GF/C was applied to estimate $a_p(\lambda)$ according to Equation 8. The present procedure provides an algorithm for direct estimate of $OD_s(\lambda)$ from measurement of $OD_f(\lambda)$ for various filter types.

Comparisons of $a_p(\lambda)$ determined from measurement of $OD_s(\lambda)$ using the integrating sphere, and estimates using the new direct algorithm for GF/F or the previous indirect procedure are provided for a culture and a sea water sample in Figure 5a and 5b, respectively. The sea water sample was concentrated by filtration and resuspended for determination of $OD_s(\lambda)$. Small volumes of the concentrated suspension (1-10 ml) were filtered onto GF/F filters for $OD_f(\lambda)$ measurements.

Estimates of $a_p(\lambda)$ using the previous algorithm are as low as 75% of the estimates using the new algorithm. Analysis of the source of the variability indicates that the relationship previously used to estimate $OD_f(\lambda)$ for GF/C from $OD_f(\lambda)$ GF/F is responsible for most of difference. Previously[2,16], linear regressions of $OD_f(\lambda)$ for GF/F as the dependent variable and $OD_f(\lambda)$ for GF/C as the independent variable resulted in a slope of 1.3. In the present study, the slope was 1.14. The previous algorithm for GF/C provides estimates which are approximately 90% of the estimate of the new algorithm for GF/C, which is within the precision of the QFT. Thus it appears that variation between the algorithms is due to the conversion from GF/F to GF/C using the previous indirect method. It appears that different filter lots cause variability in the algorithms of $\pm$ 15%.

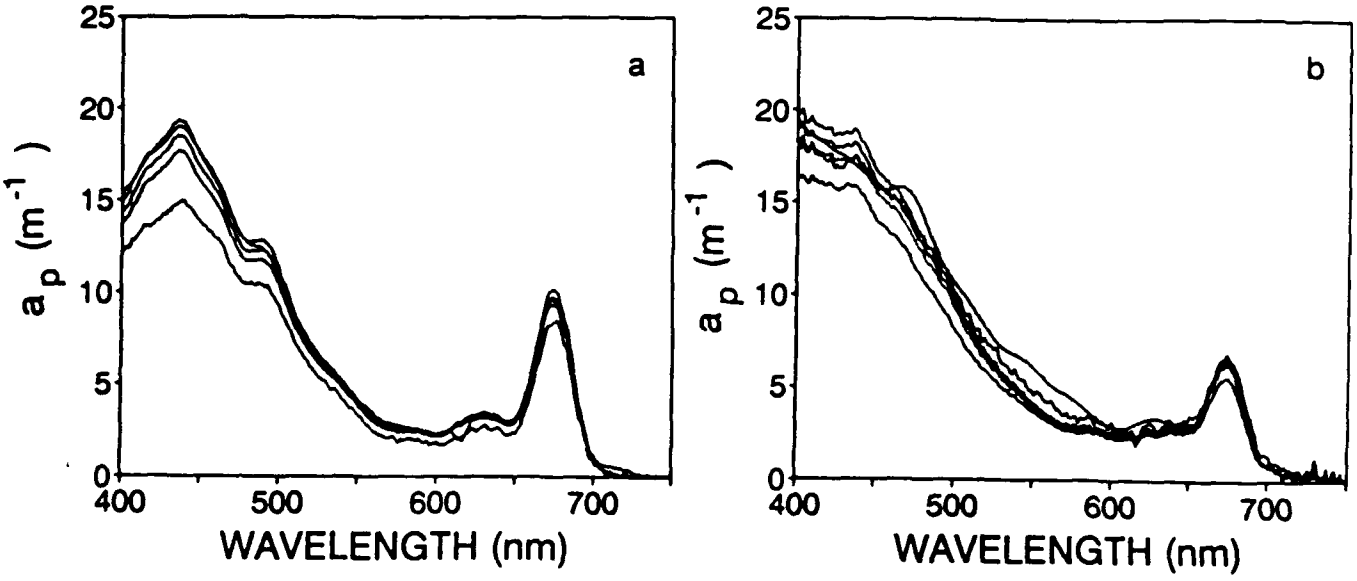

Figure 5. Comparison of estimates of $a_p(\lambda)$ using the integrating sphere, the recommended algorithm ± the 95% confidence interval for the GF/F filter type, and the previous, indirect method for GF/F. (a) Results for a culture of *Thalassiosira fluviatilis*. (b) Results for concentrated sea water collected from Scripps Institution of Oceanography pier. Results of the previous algorithm (lowest curve in each plot) underestimates $a_p(\lambda)$ by 15-25% compared to either the current algorithm or the integrating sphere observations on suspensions.

This magnitude of variability between algorithms is greater than the precision determined in the analysis of variability of replicates of $OD_f(\lambda)$ measured with different post-sample acceptance angles (Figure 1). Volume measurement errors are expected to be approximately 5% and errors in distribution of particles on the filter are probably of similar magnitude. Given these uncertainties, the QFT appears to have an overall precision of ± 10%. Error in curve fitting relationships between $OD_s(\lambda)$ and $OD_f(\lambda)$ on specific lots of filters results in an additional 5% error. Thus, the overall accuracy of the procedure is of the order ± 15 provided the curve fit is for the filter lot used. However, an additional error of comparable magnitude may be caused by variations between filter lots, and if this is not considered, the aggregate error may be as great as 20-30 %.

2.4 Variations among filters types

It is not possible to use a single algorithm for the QFT for samples concentrated on different filter types. Differences among filter types have been reported[2,16] and were attributed to variations in the intensity of scattering due to filter characteristics (thickness, density of weave, diameter of fibers, etc.). A direct comparison between filter types, using cultures of *D. tertiolecta*, *Chlorella sp.* and *T. fluviatilis* was carried out. The data used for this analysis are a subset of the total data set for which the same volume of the cultures were determined for all of the four filter types. For each species, $OD_s(\lambda)$ was determined on a dilution of the culture so that the maximum $OD_s(\lambda)$ in a 1 cm cuvette was

between 0.05 and 0.1. Several volumes covering a 10-fold range were filtered onto the different filter types. The original $OD_s(\lambda)$ determined in a 1 cm cuvette was scaled by l_g for the various volumes filtered. A quadratic equation fit to the data was made for each filter type and a summary of the results are presented in Figure 6. In Figure 6a, the best fit curve of $OD_s(\lambda)$ as a function of $OD_f(\lambda)$ for each filter type is shown. Figure 6b demonstrates that β is a non-linear function of $OD_f(\lambda)$ and is different for the various filter types. The best fit coefficients for this analysis are presented in Table 2. The best fit coefficients for GF/C and GF/F are slightly different than those for the larger data set presented in Table 1. However, in the range of $OD_f(\lambda)$ from 0.05 to 0.4, the two fits predict $OD_s(\lambda)$ within 10% which is considered to be the overall precision of the QFT.

Highest values of β were observed for the 934AH filter type. This is a surprising result and does not agree with previous observations[2,16]. This may be attributable to a lower tolerance for its manufacturing specification compared to the other filter types. The allowable manufacturing tolerance for range in thickness, as a fraction of the mean thickness, is 0.46, 0.26, and 0.27 for the 934AH, GF/C, and GF/F filters types, respectively (E. Heilweil, Whatman, Inc. technical service, personal communication). The magnitude of β is expected to increase with increased thickness of the filter. Previously, the Millepore HA filter was determined to have the highest β. Now, the HA type is between the GF/F and the GF/C. As previously discussed[2,16], the HA filter type is difficult to use because it is not as hygroscopic as the glass filter types. Thus it is difficult to keep saturated with water unless a portion is actually immersed in fluid. This was not possible using the mounting procedure previously used, but the present method did maintain saturation. The present algorithm for HA is therefore considered more accurate, provided the sample and reference filters are kept saturated during the analysis. The relationship for the GF/C filter type is similar to previous results.

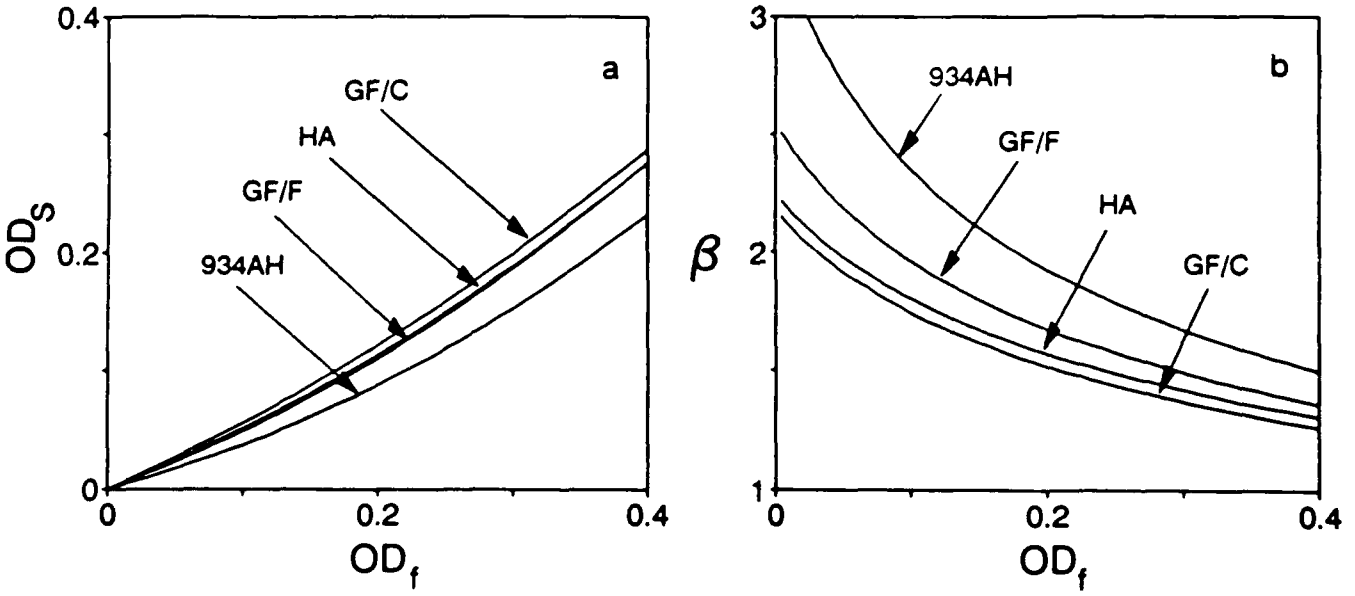

Figure 6. Comparison of algorithm results for Whatman glass fiber filter types GF/C, GF/F and 934AH and Millepore cellulose acetate type HA. (a) Curves for the best fit of the quadratic equation for the relationship between $OD_s(\lambda)$ and $OD_f(\lambda)$ for experiments conducted with *Dunaliella tertiolecta*, *Chlorella sp.* and *Thalasiossira fluviatilis*. Quadratic equation best fit coefficients are from Table 2. (b) The relationship between β and $OD_f(\lambda)$ for the best fit relationships presented in Figure 6a.

		GF/F	GF/C	934AH	HA
n observations		2800	2800	2800	2800
a	95% lower	0.407	0.491	0.286	0.430
	estimate	0.415	0.500	0.298	0.445
	95% upper	0.422	0.509	0.309	0.460
b	95% lower	0.665	0.516	0.663	0.560
	estimate	0.690	0.547	0.706	0.611
	95% upper	0.714	0.577	0.750	0.663

Table 2. Coefficients for the quadratic equation fit (Equation 9) of the limited studies of the relationship between $OD_s(\lambda)$ and $OD_f(\lambda)$ for Whatman GF/C, GF/F, 934AH and Millepore HA filter types. The best estimate and the 95% confidence interval for the coefficients a and b are provided.

2.5 Recommended procedure

Unlike the term β in Equation 8, the coefficients a and b in Equation 9 have no physical significance. Nevertheless, predicting $OD_s(\lambda)$ from $OD_f(\lambda)$ using the quadratic equation approach is more direct. Furthermore, estimates of β are subject to compounded errors by taking the ratio of experimentally determined values of $OD_s(\lambda)$ and $OD_f(\lambda)$ in the algorithm development. Thus, when using Equation 8 as previously recommended[1,2,16] estimates of $OD_s(\lambda)$ will be subject to uncertainty in both the experimentally determined $OD_f(\lambda)$, and the compounded error in estimates of β. Errors in β are of greatest concern at low values of $OD_f(\lambda)$ where instrumentation noise and baseline correction errors become a more significant part of the signal. To minimize error in the curve fitting, it is better to fit the relationship between $OD_s(\lambda)$ and $OD_f(\lambda)$ rather than the relationship between β $(OD_f(\lambda)/OD_s(\lambda))$ and $OD_s(\lambda)$. Once a fit is obtained, it can be solved for β, if desired (Figures 2, 4b, 6b) . It is therefore recommended that estimates of $a_p(\lambda)$ be based on a direct estimation of $OD_s(\lambda)$ from experimentally determined values of $OD_f(\lambda)$ using the quadratic equation fit procedures outlined above. From $OD_s(\lambda)$, $a_p(\lambda)$ can be calculated:

$$a_p(\lambda) = 2.3\ OD_s(\lambda) / l_g \tag{10}$$

Some practical considerations should also be mentioned. Unsatisfactory filtration results, due to clogging, have been obtained using filtration devices with a fritted glass support for the filter. Better results are obtained with filtration devices which have either stainless steel or plastic screens supporting the filter. Once filtered, samples should be kept saturated and refrigerated in the dark until analyzed.

Previous experiments[16] indicated no significant loss of absorption for filtered samples of a culture kept at 4 °C for up to 24 hours, but changes might be species specific depending on pigment degradation enzymes and other factors. Significant loss of absorption (up to 25%, particularly in the red peak) and spectral shifts in the blue have been observed for filtered samples kept frozen for 6 months at -20 °C in air (B. G. Mitchell, unpublished data). Until a satisfactory procedure can be demonstrated for long-term storage of samples, it is strongly recommended that analyses be done as soon as possible after sampling.

Treatment of baseline offsets is also an important consideration. In general, the baseline is spectrally flat, although it can vary by $OD_f(\lambda) = \pm 0.03$. This is of no consequence provided a wavelength with no absorption is available as a null reference. For cultures such as those studied here, the assumption of no absorption at 750 nm is reasonable. However, this assumption poses problems in field work, particularly if a significant fraction of the particulates are of detrital origin. Nevertheless, considering baseline shifts of $OD_f(\lambda) \pm 0.03$, the magnitude of error if a 750 nm null correction is not used would be greater than the errors associated with implementation of the usually reasonable assumption that absorption at 750 nm is zero.

3. CONCLUSIONS

A detailed analysis was conducted regarding the generality, accuracy and precision of the quantitative filter technique (QFT) for determining the absorption coefficient of aquatic particulates, $a_p(\lambda)$. The generality of the procedure was verified through the observation that changing the angle of acceptance to the detector of the post-sample diffuse light did not significantly alter the magnitude of $OD_f(\lambda)$, provided the baseline was properly determined. The QFT is capable of estimating the magnitude of $a_p(\lambda)$ with a precision of better than 10% and an overall accuracy within $\pm$ 15 %. This accuracy is attained if coefficients for a specified lot of filters are determined. The non-linearity between β and $OD_f(\lambda)$ was verified as was the difference in β for different filter types.

A new, more direct, algorithm for the GF/F filter type results in 15-25% higher estimates of $a_p(\lambda)$ compared to the previous indirect method of converting $OD_f(\lambda)$ for GF/F to $OD_f(\lambda)$ for GF/C and then correcting with β for the GF/C. Although the GF/C and GF/F filter types appear to be more consistent with previous observations, a difference in the slope of linear fits between $OD_f(\lambda)$ for GF/F and GF/C, compared to previous observations[2], is hypothesized to be caused by variations in filter lots. The higher slope previously observed results in an overcorrection when applied to analyses with the current stock of filters. Results in this study for the 934AH filter type were significantly different than previous results[2,16]. Apparently, filters from different lots have different thickness which may cause different relationships for β. If these differences are not considered, an additional error of 10-15 % beyond the accuracy of the procedure may result. For the highest possible accuracy of the QFT, it may be necessary to determine the coefficients for each lot of filters used.

4. ACKNOWLEDGEMENTS

This research was supported by the Office of Naval Research Ocean Optics program (Grant N00014-89-J-1071). The invaluable assistance of Eric Brody and Vinnie Spode in programming, data analysis, statistical curve fitting and graphics preparation is gratefully acknowledged. I thank Drs. F. T. Haxo and R. Lewin for inocula of cultures; Dr. A. Weidemann for useful discussions and laboratory assistance; and Dr. M. Vernet and H. Sosik for comments on a draft of the manuscript.

5. REFERENCES

1. B. G. Mitchell, and D. A. Kiefer "Determination of absorption and fluorescence excitation spectra for phytoplankton. In: Marine Phytoplankton and Productivity, O. Holm-Hansen, L. Bolis, and R. Gilles editors, Springer-Verlag, Berlin, New York. pp. 157-169, 1984.

2. B. G. Mitchell and D. A. Kiefer, "Chlorophyll a specific absorption and fluorescence excitation spectra for light-limited phytoplankton," Deep-Sea Research, vol. 35, pp. 639-663, 1988.

3. R. W. Preisendorfer, Hydrologic Optics , U. S. Department of Commerce, National Oceanic and Atmospheric Administration, Environmental Research Laboratory, 1976.

4. H. R. Gordon, R. C. Smith and J. R. V. Zaneveld, "Introduction to Ocean Optics" In: Ocean Optics VI, M. Blizard editor, SPIE, Bellingham, WA. pp. 14-55, 1979.

5. A. Morel and L. Prieur, "Analysis of variations in ocean color," Limnology and Oceanography, vol. 22, pp. 709-722, 1977.

6. C. S. Yentsch, "Measurement of visible light absorption by particulate matter in the ocean," Limnology and Oceanography, vol. 7, pp. 207-217, 1962.

7. D. A. Kiefer and J. B. Soo Hoo, "Spectral absorption by marine particles of coastal waters of Baja California," Limnology and Oceanography, vol. 27, pp. 492-499, 1982.

8. W. L. Butler, "Absorption of light by turbid materials," Journal of the Optical Society of America, vol. 52, pp. 292-299,1962.

9. B. G. Mitchell, R. Iturriaga and D. A. Kiefer, "Variability of particulate spectral absorption coefficients in the Eastern Pacific Ocean," In: Ocean Optics VII, M. Blizard editor, SPIE, Bellingham, WA. pp. 113-118, 1984.

10. M. Kishino, N. Takahashi, N. Okami and S. Ichimura, "Estimation of the spectral absorption coefficients of phytoplankton in the sea," *Bulletin of Marine Science*, vol. 37, pp. 634-642, 1985.

11. M. R. Lewis, R. E. Warnock and T. Platt, "Absorption and photosynthetic action spectra for natural phytoplankton populations: Implications for production in the open ocean," Limnology and Oceanography, vol. 30, pp. 794-806, 1985.

12. B. G. Mitchell and D. A. Kiefer, "Variability in pigment specific particulate fluorescence and absorption spectra in the North Eastern Pacific Ocean," Deep-Sea Research, vol. 35, pp. 665-689, 1988.

13. C. S. Yentsch and D. A. Phinney "The use of the attenuation of light by particulate matter for the estimate of phytoplankton chlorophyll with reference to the coastal zone color scanner," Journal of Plankton Research, vol. 4, pp. 93-102, 1982.

14. D. A. Kiefer, R. J. Olson and W. H. Wilson, "Reflectance spectroscopy of marine phytoplankton. Part 1. Optical properties as related to age and growth rate," Limnology and Oceanography, vol. 24, pp. 664-672, 1979.

15. J. T. O. Kirk, "Spectral properties of natural waters: Contribution of the soluble and particulate fractions to light absorption in some inland waters of southeastern Australia," Australian Journal of Marine and Freshwater Research, vol. 31, pp. 287-296, 1980.

16. B. G. Mitchell, Ecological implications of variability in marine particulate absorption and fluorescence excitation spectra, Ph.D. Thesis, The University of Southern California, Los Angeles, California, 196 pp, 1987.